https://doi.org/10.5194/egusphere-2026-3846
Preprint. Discussion started: 8 July 2026

Ice core insights into the morphology and composition of mineral dust deposited in the tropical Peruvian Andes

Austin M. Weber[1,2], Stanislav Kutuzov[1,2], Emilie Beaudon[1,2], M. Roxana Sierra-Hernández[3], Mary Davis[2], Laurel H. Bayless[4,5], Don Kenny[2], and Lonnie G. Thompson[1,2]

[1]School of Earth Sciences, The Ohio State University, Columbus, 43210, USA
[2]Byrd Polar and Climate Research Center, Columbus, 43210, USA
[3]Department of Physical & Environmental Science, Texas A&M University—Corpus Cristi, Corpus Cristi, 78412, USA
[4]Department of Earth Science, University of Colorado—Boulder, Boulder 80303, USA
[5]Institute of Arctic and Alpine Research, University of Colorado—Boulder, Boulder 80309, USA

Correspondence to: Austin M. Weber (weber.1158@osu.edu)

Abstract. Mineral dust plays an important role in governing Earth's energy balance by scattering electromagnetic radiation back to space and by reducing the surface albedo of glaciers. However, in the tropical Andes of South America, long-term mineral dust observational records are extremely scarce and spatially limited; likewise, little has been done to characterize the morphological and mineralogical properties of dust in this region. Here we present a multidecadal mineral dust record obtained from a tropical ice core with emphasis on the size distributions, shape characteristics, and mineral compositions of single particles. We used a scanning electron microscope with energy dispersive x-ray spectrometry (SEM-EDS) to characterize 1887 individual mineral grains (<5 μm) preserved in an ice core from Nevado Huascarán (Peru) and we interpret the results in context of dust provenance. The SEM-derived particle sizes are found to follow a lognormal distribution with circularities (median 0.75) and aspect ratios (median 1.42) typical of mineral dust. Approximately 60% of the mineral particles are consistent with clay mineralogy (e.g., illite, kaolinite, montmorillonite), indicating that the particles originate primarily from soils in distal source areas. The relative abundance of quartz, feldspar, and mica in the ice core is comparatively low and likely reflects local dust derived from granodiorites and phyllites near the glacial margins.

1 Introduction

The sizes, shapes, and composition of mineral dust particles influence their radiative properties (Gieré and Querol, 2010; Highwood and Ryder, 2014) and affect their settling velocities during transport (Gieré and Querol, 2010; Li and Osada, 2007; Pye, 1994). Mineral dust increases planetary albedo by scattering electromagnetic radiation back into space, with a net cooling effect of approximately -0.2 ± 0.5 W m^{-2} (Kok et al., 2023). However, not all minerals contribute to cooling. For example, iron oxides (such as hematite) act as energy absorbers (Gonçalves Ageitos et al., 2023). When deposited onto glaciers, mineral dust lowers the albedo of the surface snow and promotes negative mass balance changes (Dang et al., 2015;

https://doi.org/10.5194/egusphere-2026-3846
Preprint. Discussion started: 8 July 2026

Di Mauro et al., 2024; Painter et al., 2007; Shi et al., 2021; Warren, 1984). Particle mineralogy plays a critical role in governing the relative reduction in glacial albedo (e.g., Flanner et al., 2021).

Dust deflation models, atmospheric models, energy balance models, and radiative transfer models used in cryosphere research rely on morphological and mineralogical assumptions or approximations in order to simulate the behaviour of mineral dust and its impacts (e.g., Flanner et al., 2021; Gassó et al., 2010; Tegen and Schulz, 2014). However, the parameterizations made in these model frameworks are not always realistic or are poorly constrained due to the scarcity of relevant observational data. For instance, many legacy models assume that particles can be approximated as spheres or that the particles have a homogeneous or an invariable composition (Engelbrecht and Derbyshire, 2010). The need for improved mineral dust data sets is therefore well known (Buseck, 2010).

In the tropical Andes of South America, observational mineral dust records are severely limited both spatially and temporally (Gilardoni et al., 2022). The impact of mineral dust in this region, specifically with respect to mountain glaciers, has potentially significant social and economic implications. For instance, the loss of glaciers can have a profound spiritual effect on indigenous communities (Allison, 2015). Glacier melting also increases the risk of glacial lake outburst floods (GLOFs) capable of decimating pastures, villages, and urban population centers (Carey, 2005; Carrivick and Tweed, 2016; Emmer et al., 2022; Stuart-Smith et al., 2021; Taylor et al., 2023). Mountain communities are also heavily reliant on the glaciers for freshwater, and therefore the loss of glaciers in the region triggers an array of water resource issues ranging from decreased water availability for irrigation and diminished hydropower (Chevallier et al., 2011; Thompson et al., 2021).

To improve our understanding of the physical nature of dust in the tropical Andes, we use a scanning electron microscope with energy dispersive x-ray spectrometry (SEM-EDS) to thoroughly examine the mineral dust preserved in a Peruvian ice core. Ice cores provide valuable insights into the morphology and composition of mineral dust (Wu et al., 2016) and also illuminate important details about dust over extended periods of time (Nagatsuka et al., 2021). However, very little has been done to characterize the shapes, sizes, and composition of dust in ice cores from the tropics, even though there have been many deep ice core records collected from low latitude glaciers (e.g., Permana et al., 2019; Ramirez et al., 2003; Thompson et al., 1995, 1998, 2002, 2013). To our knowledge, this is the first study to report a multidecadal history of mineral dust preserved in a tropical ice core and the first to present detailed morphological and compositional data on the physical properties of dust in this part of the world.

2 Study region

The Cordillera Blanca mountain range (in the north-central Peruvian Andes; Fig. 1) contains 25% of all tropical glaciers on Earth (Glas et al., 2018; Kaser et al., 2003). The Cordillera Blanca is also home to the world's highest tropical mountain,

https://doi.org/10.5194/egusphere-2026-3846
Preprint. Discussion started: 8 July 2026

Nevado Huascarán (9.11°S, 77.61°W), the mountain col of which sits at 6050 meters above sea level (m a.s.l.). The recovery of ice cores from the col of Huascarán in 1993 (Thompson et al., 1995) and again in 2019 (Kutuzov et al., 2025) allowed researchers to study the climatological history of the region with respect to coupled ocean-atmosphere systems (such as the El Niño-Southern Oscillation; e.g., Henderson et al., 1999; Weber et al., 2023), but very little has been done to characterize the morphology and composition of mineral dust preserved in the ice core records.

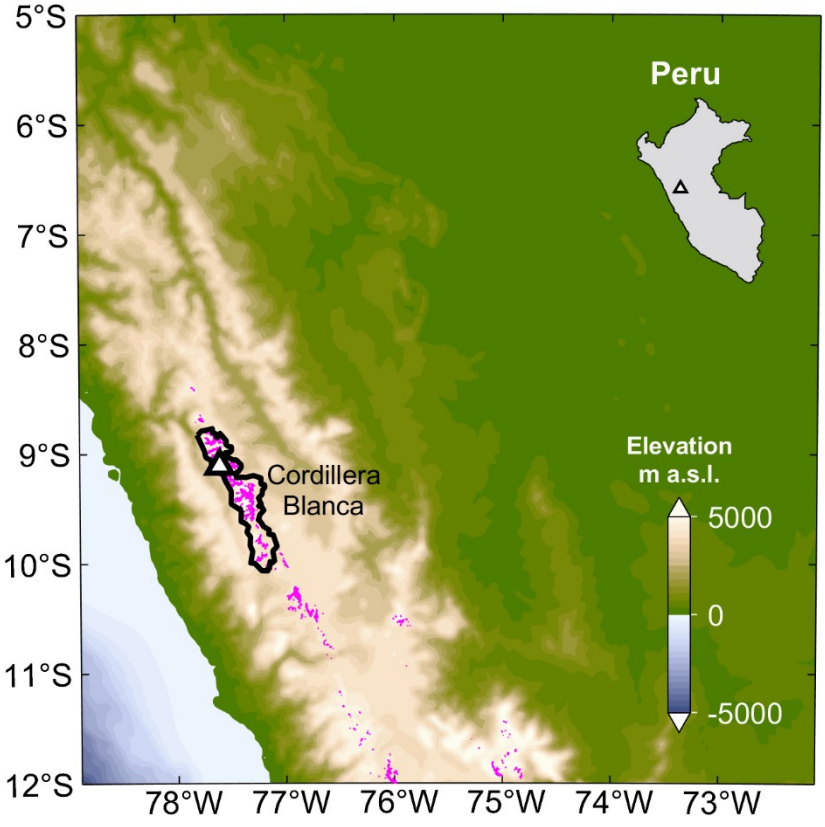

Figure 1. Map of the study region. Elevation data were acquired from ETOPO2 (NGDC, 2001) and are visualized using the M_Map software for MATLAB® (Pawlowicz, 2020). Magenta pixels show the locations of low-latitude glaciers (RGI Consortium, 2023). The white triangle marks the location of Nevado Huascarán (9.11°S, 77.61°W).

During the austral summer (November–April), the zonal wind direction and the southerly position of the intertropical convergence zone (ITCZ) promote the transport of dust originating in North Africa to the Amazon Basin via the Saharan Air Layer (Prospero et al., 2021). Dust deposited over the eastern Amazon during this time is responsible for replenishing the soils with micronutrients (Bristow et al., 2010). At the same time, the South America monsoon system (SAMS) inundates the Amazon Basin with rainfall while moisture recycling pathways propagate across the tropical forests (Zemp et al., 2014). Wet season conditions related to the SAMS are likely to remove most, if not all, of the African-sourced dust from the atmosphere

https://doi.org/10.5194/egusphere-2026-3846
Preprint. Discussion started: 8 July 2026

before it reaches the tropical Andes. However, some studies have shown that African dust is capable of being carried as far as Colombia and Ecuador (Bolaño-Ortiz et al., 2023; Boy and Wilcke, 2008) and to the equatorial Pacific on millennial time scales due to shifts in the ITCZ (Schimmenti et al., 2025).

The austral winter (May–October) is the dry season in the Cordillera Blanca when rainfall amounts are less than 10% of the annual total (Vuille et al., 2008). At the same time, the ITCZ shifts to the north and redirects the transport of dust from Africa towards the Caribbean and southern United States (Prospero et al., 2021). During the dry season dust concentrations peak in the Huascarán ice core record (approximately 3-times higher than wet season levels on average); however, average grain sizes and dust size ratios are similar between the wet and dry seasons (Davis, 2002). While there is likely some increased dust deposition during the austral winter due to reduced snow cover and a corresponding increase in the availability of local dust, the pronounced dry season peak in dust concentrations is primarily the result of the decreased snowfall rate in tandem with lower cloud cover and high solar irradiance. These conditions enhance the rate of ablation at the ice core site and therefore concentrate dust that was deposited during the preceding summer months (Davis, 2002).

It has been hypothesized that recent changes in forest cover within the Amazon may play a role in the generation and transport of dust to Huascarán (Davis, 2002; Weber et al., 2026a); however, direct evidence of this relationship has yet to be shown. The idea is supported by the work of Tegen and Fung (1995) and Tegen et al. (1996), who show that 50 ± 20% of global dust emissions are related to the disturbance of soils. Since the 1970s, nearly 20% of Amazonian forests have been removed and/or burned for urbanization and the expansion of farmland (Bullock et al., 2020; Fearnside, 2005; Mu and Jones, 2022), which has reduced surface roughness and exposed bare sediments within the basin. Betts et al. (2008) modeled future dust emissions within the Amazon and showed that significant changes in forest cover may eventually lead to massive regional dust emission rates. Estimates of the Amazon rainforest's "tipping point" suggest that a forest dieback and savannization scenario may already be underway (Lovejoy and Nobre, 2018; Poveda, 2026; Restrepo-Coupe et al., 2023). Satellite observations show that during the dry season aerosols in the Amazon Basin are lifted in significant amounts over the Andes towards the Pacific ocean (Bourgeois et al., 2015).

Other potential dust sources in tropical South America include the high Puna-Altiplano deserts, with regular sand and dust storms originating from the Salar de Uyuni (southern Altiplano, Bolivia) and the Salinas Grandes (northern Puna, Argentina) throughout the year (Gaiero et al., 2013), as well as coastal Peru, where 4–5 dust storms per year have been documented (Briceño-Zuluaga et al., 2017).

Mineral dust that is generated locally (i.e., within the Cordillera Blanca) is related to the geology of the mountain range. The batholith is primarily composed of sodium-rich granodiorites and tonalites from the Neogene-Miocene (Atherton and Petford, 1993; Atherton and Sanderson, 1987; Petford and Atherton, 1996), which by definition include plagioclase, quartz,

https://doi.org/10.5194/egusphere-2026-3846
Preprint. Discussion started: 8 July 2026

and alkali feldspar. Minor amounts of biotite, hornblende, and muscovite are also found in these plutonic rocks (Atherton and Sanderson, 1987). To the east of Huascarán is the Chicama Formation, which is primarily composed of Jurassic-age metasedimentary deposits (Giovanni et al., 2010; Glas et al., 2018). The weathering and erosion of these rocks is a potential source of phyllosilicate minerals, particularly mica and illite. Granodiorite, tonalite, and Chicama materials are currently being exposed by the retreat of glaciers in the Cordillera Blanca. For example, according to recent satellite-derived measurements, the total ice extent on Huascarán changed by −21% between 1987 and 2020 (Schoessow, 2025). Glacier recession and snow season shortening increases the frequency and probability of dust emissions in glacierized environments (Meinander et al., 2022). Relatedly, the exposure of subglacial sediments due to glacier retreat within the Cordillera Blanca has been linked to downstream effects in water quality (Fortner et al., 2011; Magnússon et al., 2020).

3 Methodology

3.1 Sample selection

The ice cores recovered during the 2019 drilling campaign on the Huascarán col are annually resolved through the most recent six decades (Weber et al., 2023), although lower-confidence annual records can be extended back to 1720 CE with a dating uncertainty of approximately ±5 y (Davis, 2002). In this study we examine single particles preserved in the uppermost 80 meters of the 2019 Huascarán Col A ice core (HC-19A) to gain insights into the nature of dust between 1960 and 2018 CE.

Using a precleaned bandsaw, we subsampled HC-19A in the cold room laboratory at the Ohio State University's Byrd Polar and Climate Research Center (OSU-BPCRC) to acquire samples (2.6×2.6×2.6 cm^3) corresponding to the annual dust maxima of the last 60 y (Fig. 2). The ice samples were immediately transferred to the Class 100 clean room at OSU-BPCRC in pre-cleaned capped plastic cups. Firn-layer samples were cut from the core at slightly larger volumes so that enough sample would be available for the decontamination procedure. Considering that contamination in firn is limited to the outer 3–6 mm of the core (Osterberg et al., 2006), we used precleaned steel chisels to scrape and/or chisel the outermost ~5 mm of the firn under a laminar flow hood within the cold room. Like the ice samples, the decontaminated firn samples were transferred to the Class 100 clean room in capped plastic cups.

https://doi.org/10.5194/egusphere-2026-3846
Preprint. Discussion started: 8 July 2026

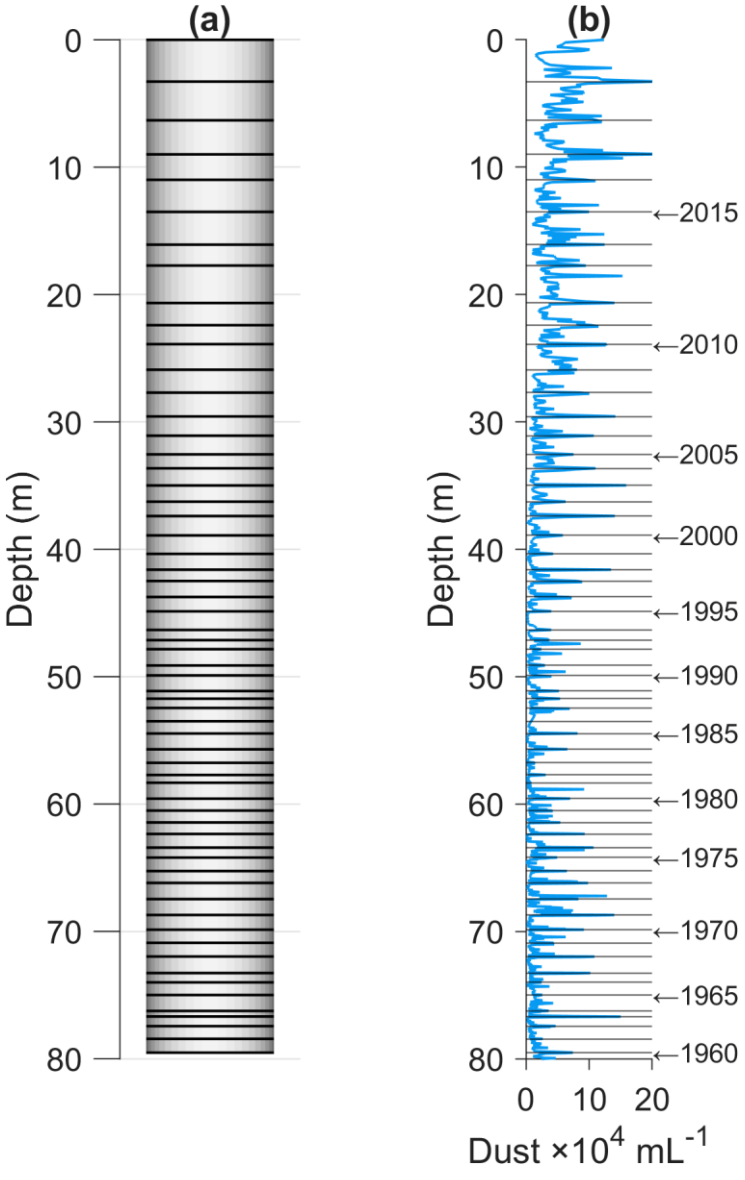

Figure 2. Dust sampling scheme for the 2019 Huascarán Col A ice core (HC-19A). (a) Schematic of the ice core with black lines showing the sampling depths. Made with the Core Stratigraphy Visualization tool in MATLAB® (https://www.mathworks.com/matlabcentral/fileexchange/173320-core-stratigraphy-visualization). (b) Microparticle concentrations as a function of depth, determined by Coulter Counter. Black horizontal lines denote the sampling depths for this study with annual labels every fifth year.

https://doi.org/10.5194/egusphere-2026-3846
Preprint. Discussion started: 8 July 2026

3.2 Sample preparation

To decontaminate the ice samples, their outer surfaces were rinsed using 18.2 MΩ ultrapure water. All decontaminated firn and ice samples were allowed to melt in precleaned cups, and the meltwater from the cups was used to isolate the microparticle contents onto 25 mm 0.1 µm Isopore™ polycarbonate membranes using glassware fitted for vacuum filtration.

Twelve dust filters were prepared for SEM-EDS by combining the meltwater samples in five-year intervals (e.g., 1960-64, 1965-69, …, 2015-2018). The consolidation of the 59 annually dated samples into 12 multiannual samples was necessitated by time and monetary constraints while still allowing us to collect data on at least 150 particles per sample (i.e., the minimum number of particles recommended for an ice core SEM-EDS analysis; Nagatsuka et al., 2021).

The 12 dust filter samples were adhered to individual 25 mm SEM pin mounts using double-sided carbon tape and stored in the clean room until time for analysis. On the day of analysis for each sample, the filters of interest were transported to the Center for Electron Microscopy and Analysis (CEMAS) in SEM storage boxes wrapped in Parafilm. At CEMAS, the samples were coated with a thin layer (10–20 nm) of vaporized carbon using a sputter coater (Leica EM ACE600). The carbon coat limits charging effects during SEM analysis by increasing the conductivity of the sample surface (Goldstein et al., 2003).

3.3 Particle analysis by SEM-EDS

We used the Quattro Environmental SEM at CEMAS to analyze the mineral dust contents of the 12 filter samples. The instrument is equipped with an EDAX Octane Elect Super 70 mm^2 EDS detector, which was used for the collection of x-ray energy spectra for each particle of interest.

The following SEM operating conditions were determined to be optimal for the analysis: 15 kV acceleration voltage, 2.8 nA beam current, and 12 mm working distance. Using the DTSA-II software from the National Institute of Standards and Technology (NIST, http://www.nist.gov/dtsa), we performed a bulk Monte Carlo simulation to estimate the interaction volume of the electron beam under these operating conditions. The simulated penetration depth of the electron beam was 0.76–2.29 µm with an interaction volume of 0.81–15.97 $µm^3$. To avoid the generation of mixed x-ray signals, we focused our analysis on isolated particles and particles exhibiting minimal overlap with adjacent particles. We also attempted to select these particles at random, but because this was done manually the analysis may have been subject to some human bias. Likewise, we tried to limit our analysis to particles less than 5 µm in diameter so that our mineralogical conclusions would not be biased by the local dust signal. Because the Huascarán col is more than 6000 m a.s.l., coarse particles are most likely derived from local sediments, whereas smaller size fractions are representative of both local and distal dust.

https://doi.org/10.5194/egusphere-2026-3846
Preprint. Discussion started: 8 July 2026

A backscatter electron image was saved for every probed particle along with the particles' x-ray energy spectrum, obtained via energy dispersive spectrometry (i.e., with the EDS detector). We collected EDS data for 10 s live time on each particle, which was sufficient to produce a well-resolved EDS spectrum in most cases. Any poorly resolved spectra were discarded during the data processing stage because mineralogy could not be reasonably inferred. Poor spectra may have resulted from a particle being too low-mass to generate enough x-rays or by a larger adjacent particle that blocked x-rays from reaching the detector.

3.4 Quantifying particle morphology

The morphologies (referring to size and shape characteristics) of the individual particles were quantified using the image processing software Fiji (Schindelin et al., 2012), in which the scale bar in each backscatter electron micrograph was used to set the pixel width of the images. Individual particles were traced using a stylus on a touchscreen computer to ensure that their perimeters were accurately defined. Binary masks were generated for each relevant particle, and the Analyze Particles tool in Fiji was used to calculate the two-dimensional area, circularity, and aspect ratio of every masked particle. In order to evaluate size distribution statistics on the bulk samples in a standardized manner, the equivalent circular diameter (ECD) of each particle was estimated using Eq. (1).

$$ECD = 2 \times \sqrt{(Area/\pi)} \quad (1)$$

It should be noted, however, that our two-dimensional image analysis of SEM micrographs may overestimate particle sizes because mineral grains preferentially settle on their largest side (Royer et al., 1983). We are also limited in our ability to measure a sufficient number of very small (<1 μm) particles with SEM, and so the size distributions determined by electron microscopy may be biased towards higher modes and do not necessarily reflect the "true" distribution that can be obtained with a three-dimensional particle counting method (e.g., Groundwater et al., 2012; see Text S1 in the Supplementary Materials).

3.5 Mineral identification

A wide variety of techniques have been used to determine the mineralogy of particles in aerosol samples using SEM-EDS, although rarely are multiple techniques combined to improve the certainty of each classification. A common procedure is to consult the dichotomous key in Severin (2004) to compare the EDS spectrum for a particle of interest to EDS spectra collected on mineral standards (e.g., Michaud et al., 2014). This technique, however, can lead to subjective mineral assignments due to the ambiguous spectral patterns exhibited by certain mineral species. In addition, the dichotomous key approach cannot be automated as an open-source procedure due to copyright restrictions. A more quantitative approach used in the literature is to compute elemental ratios from a particle's EDS spectrum and then refer to the sorting scheme chart

https://doi.org/10.5194/egusphere-2026-3846
Preprint. Discussion started: 8 July 2026

provided by Donarummo et al. (2003). This technique has been adopted in numerous ice core mineral dust studies (Donarummo et al., 2003; Nagatsuka et al., 2021; Ro et al., 2024; Wu et al., 2016); however, the sorting scheme is limited to classifying aluminosilicate minerals and has numerous "unknown" classification nodes.

Here, we use a five-algorithm cross-referencing procedure to identify the mineralogy of particles in our dust samples. Specifically, we use an EDS mineral dust classification software package for MATLAB® (Weber, 2025) that provides users with the ability to apply numerous mineral classification algorithms to their EDS data sets. The software includes a machine learning model trained to recognize a variety of minerals commonly found in dust samples, as well as functions that give users the ability to use the mineral identification workflows described in Donarummo et al. (2003), Kandler et al. (2011), and Panta et al. (2023).

All four aforementioned computerized classification algorithms were used to ascertain the mineralogy for each particle. These results were subsequently cross-referenced with one another and with the classifications obtained via the Severin (2004) dichotomous key. This approach successfully circumvents the limitations of using any one classification method on its own; and, because the approach combines both qualitative and quantitative metrics, it significantly increases the confidence of every mineral assignment.

3.6 HYSPLIT trajectory modeling

We use the desktop version of HYSPLIT v5.3.0 (Stein et al., 2015) to run trajectory model simulations for the wet and dry seasons from 2000 through 2015. The purpose of these simulations is not to definitively trace the movement of air masses to and from Huascarán but rather to help with contextualizing our interpretations of the ice core mineral dust record. We report our HYSPLIT results as ensembles of the full 16 y model assessment period.

The model simulations were constrained using meteorological data from NCEP-NCAR reanalysis (Kalnay et al., 1996). The dry season was defined as the months June–September (JJAS) for a given year; the early wet season was defined as the December of the previous year through February (DJF) for a given year; and the late wet season was defined as March through May (MAM) for a given year.

For our model simulations we used 10 d (240 h) backward trajectories starting at Huascarán (6000 m a.s.l.), as well as 10 d forward trajectories starting at the centers of the two most likely African dust source regions (i.e., El Djouf and the Bodélé depression). We define El Djouf as 18–22°N and 10–3°W while we defined the Bodélé as 15–18°N and 12–18°E (Yu et al., 2020). The starting elevation for the two African dust source regions was 10 m above ground level. For all simulations, trajectories were evaluated at every sixth hour (i.e., 00, 06, 12, and 18 hours UTC). For the backward simulations, only the

https://doi.org/10.5194/egusphere-2026-3846
Preprint. Discussion started: 8 July 2026

grid cells in which at least 5% of the trajectories passed through are shown, whereas for the forward simulations the grid cells show where at least 2.5% of the trajectories pass through.

Several limitations prevent us from using the HYSPLIT simulations to thoroughly interpret the transport of dust to Huascarán. For one, the coarse resolution of the topography and the coarse spatial resolution (2.5°×2.5°) of the NCEP-NCAR reanalysis product may blur the highest frequency transport pathways. Using a data product with a finer grid resolution would likely improve the robustness of our simulations, but this would also greatly prolong the model runtimes which already average ~40 minutes per 16 y ensemble. Another limitation is that our simulations do not account for rainfall effects that would wash out particles from the atmosphere during transport. In addition, while the simulations consider vertical motion, our HYSPLIT output files are rendered in two-dimensions, meaning that we can only interpret the trajectory frequency maps with respect to horizontal motion. A more vigorous procedure is therefore needed to thoroughly model air mass transport to and from Huascarán, which is beyond the scope of this paper.

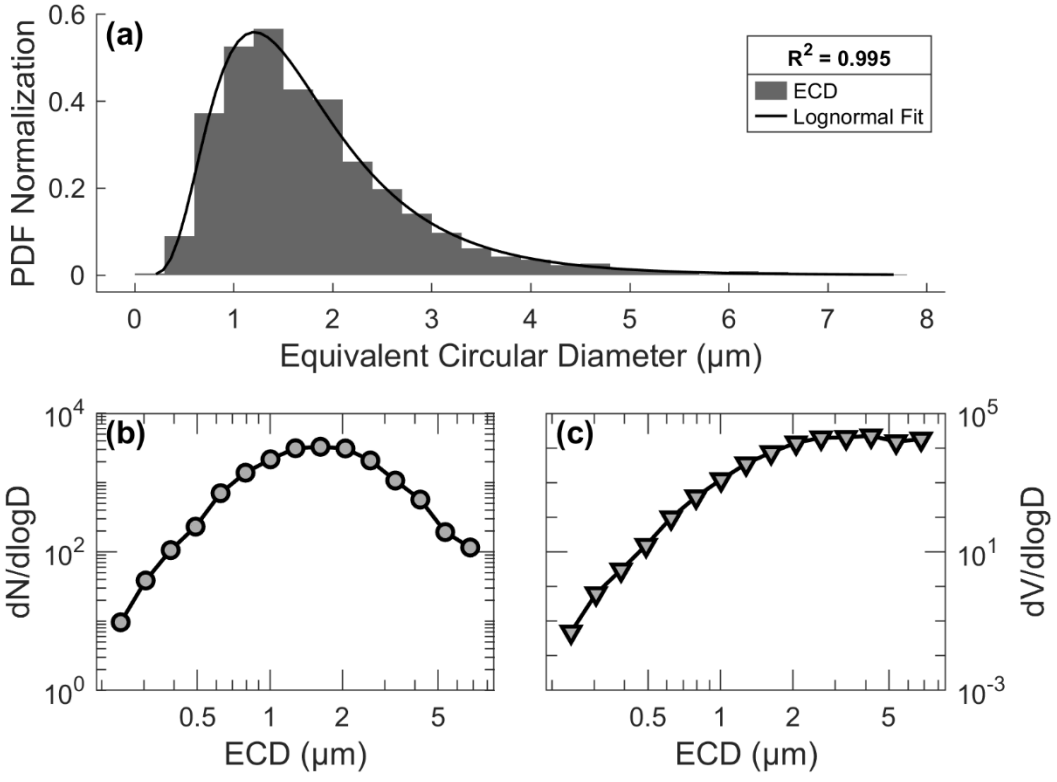

Figure 3. Particle size distributions and concentrations. (a) Histogram of the equivalent circular diameter (ECD) data with lognormal fit. (b) Particle concentrations as a function of ECD, normalized as dN/dlogD. (c) Volume concentrations as a function of ECD, normalized as dV/dlogD.

https://doi.org/10.5194/egusphere-2026-3846
Preprint. Discussion started: 8 July 2026

4 Results

4.1 Size distributions

We analyzed a total of 1887 individual mineral particles (<5 μm) in HC-19A using SEM-EDS. The size distributions of these particles are visualized in Fig. 3. The ECDs of the mineral grains display a near-perfect lognormal distribution (Fig. 3a), which is typical of aerosol samples (Blifford and Gillette, 1971); however, we note that the size distributions measured using the Coulter Counter (CC) technique are more closely described by a power-law relationship (see Text S1; Supplementary Materials), and so the size distribution results described herein are specifically interpreted in the context of what can be measured with electron microscopy.

Figures 3b-c show the concentrations of the particles normalized by the width of the size bin in log space. The dN/dlogD plot reiterates that particle sizes obtained using SEM are lognormally distributed. The mean, the median, and standard deviation of ECD are 1.8 μm, 1.6 μm, and 1.0 μm, respectively. The dV/dlogD plot reveals that larger particles dominate the total volume, despite being few in abundance. This finding is not altogether unexpected because in the formulation for spherical volume [$V=4\pi/3\times(D/2)^3$] the volume is proportional to diameter (D) cubed, meaning that a particle that is 10-times larger than average also has 1000-times more volume than average.

4.2 Particle shapes

A scatter-histogram plot of the aspect ratio versus circularity shape distributions is shown in Fig. 4. The mean and 95% confidence ellipse are shown in red. The median particle in HC-19A has a circularity of 0.75 ± 0.01 (std. error) and an aspect ratio of 1.42 ± 0.03 (std. error). The shapes of the particles in HC-19A are consistent with values reported in other aerosol studies; for example, Okada et al. (2001) and Wu et al. (2016) show that mineral dust particles in China exhibit median circularities around 0.6−0.7 and median aspect ratios around 1.4−1.5. Nagatsuka et al. (2021) examined the mineral particles in an ice core from Greenland and show median circularities around 0.7−0.8.

We use the Shapiro-Wilk parametric hypothesis test to check whether the particle shape data are normally distributed. In both cases, the null hypothesis that circularity and aspect ratio follow normal distributions is rejected at the 0.05 alpha level. For circularity, the calculated Shapiro-Wilk test statistic (W) is 0.953 (p-value < 0.0001) indicating a mild deviation from normality; for aspect ratio, W=0.795 (p-value < 0.0001) which implies a stronger deviation from normality.

https://doi.org/10.5194/egusphere-2026-3846
Preprint. Discussion started: 8 July 2026

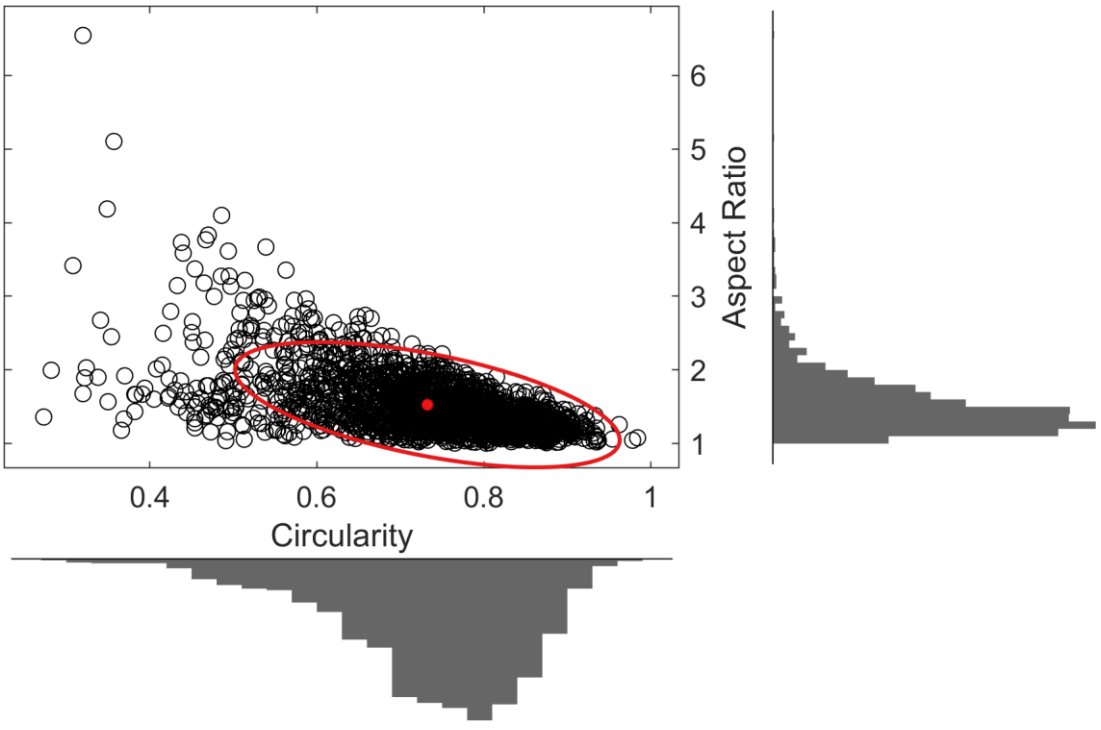

Figure 4. Scatter-histogram comparing the distributions of circularity and aspect ratio. The red dot denotes the mean of the data set; the red line is the 95% confidence ellipse.

4.3 Bulk mineralogy

Figure 5 presents the bulk mineralogical composition of HC-19A based on our SEM-EDS mineral assignments. Clay minerals are the most prevalent mineral group in the ice core by a wide margin. Five unique clay minerals were identified in the ice core record, accounting for 60.1 ± 3.0% of the total dust load. Illite is the most abundant, comprising 46.8% ± 2.0% of the clay mineral fraction, followed by kaolinite (28.6 ± 1.6%), montmorillonite (17.2 ± 1.2%), chlorite (7.0 ± 0.8%), and vermiculite (0.4 ± 0.2%). In this case, uncertainties are reported as Poisson counting uncertainties ($\sigma=\sqrt{(n)}/n_{total}$), where n is the count of particles in each group and n_{total} is the relevant total particle count.

https://doi.org/10.5194/egusphere-2026-3846
Preprint. Discussion started: 8 July 2026

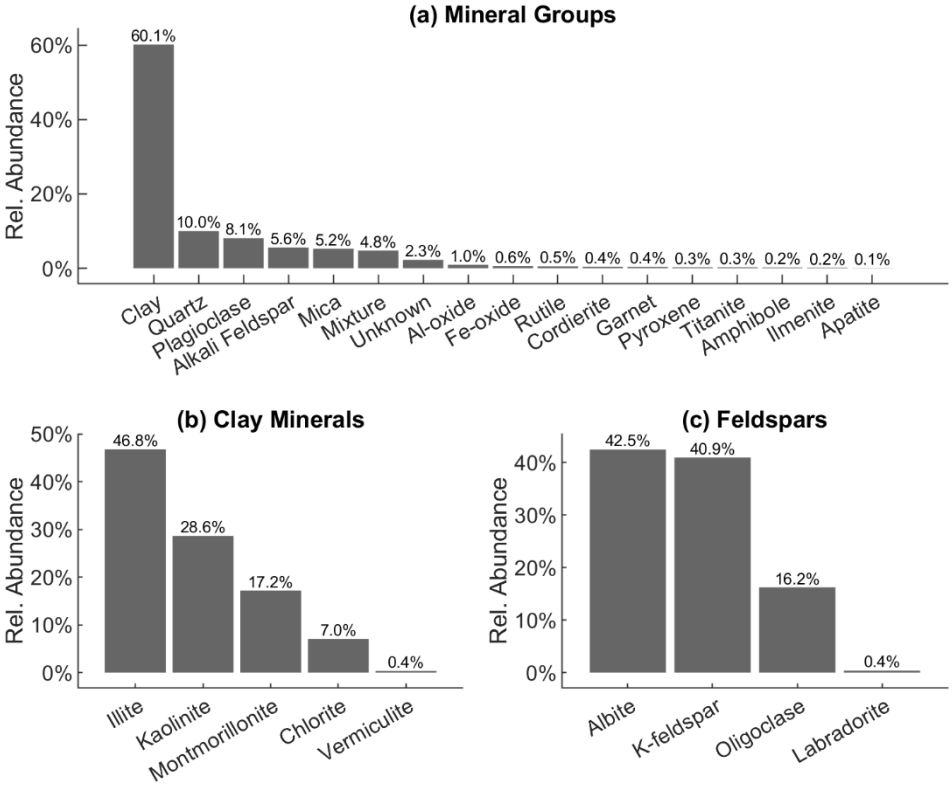

Figure 5. Bulk mineralogy histograms. (a) Relative abundance of the 17 identified mineral groups. (b) Proportions of the five clay minerals relative to one another. (c) Proportions of the four feldspar minerals relative to one another.

Feldspars (plagioclase and alkali feldspar) are the next-most abundant minerals in the ice core, accounting for 13.7 ± 0.9% of the total dust record, with plagioclase minerals (albite, oligoclase, and labradorite) representing 59.1 ± 4.8% of the feldspar fraction. The third and fourth most common mineral species are quartz (10.0 ± 0.7%) and mica (5.2 ± 0.5%), respectively. Other minerals—such as gibbsite, goethite, and rutile—were observed fewer than 20 times and thus account for only a very small proportion of the dust. Low counts among these minerals precludes them from being used in statistical testing.

4.4 Mineral morphological dependency

We tested whether mineralogy is size-dependent using one-way analysis of variance (ANOVA) (https://www.mathworks.com/help/stats/one-way-anova.html). First, the ECD data were translated into log space to meet the normality requirements of the ANOVA test. Second, only minerals with at least 30 observations were considered during the analysis in order to ensure thorough hypothesis testing. The ANOVA result for the log10(ECD) data shows that different minerals have statistically different sizes (p-value < 0.001) but the magnitude of this difference (i.e., the effect size; ω^2 =

https://doi.org/10.5194/egusphere-2026-3846
Preprint. Discussion started: 8 July 2026

0.027) suggests that mineral size dependency is very small. Mica is the only major outlier, which has a mean ECD that is statistically different than the means of 7 other minerals (Fig. 6a). Mica particles tend to be larger than other particles on average, with a mean ECD of 2.38 ± 0.13 µm (SE, n=99) compared to the ECD of the remaining minerals in Fig. 6a (1.78 ± 0.02 µm, n=1668). In any case, the mean diameter of all particles fits within the size range of the accumulation mode (0.1–2.5 µm), meaning that the larger mica particles are not necessarily biased toward local source areas.

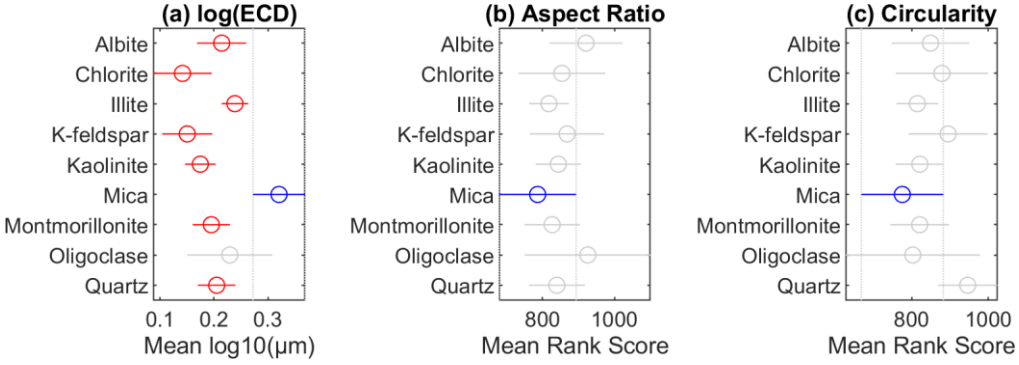

Figure 6. Multiple comparison plots for the ANOVA and Kruskal-Wallis results. Mica is highlighted in blue in all plots. Minerals highlighted in red have statistically different means than mica at the 95% level. Gray data points indicate no statistical difference in the means. (a) Results of the ANOVA for log(ECD). (b) Results of the Kruskal-Wallis analysis for aspect ratio. (c) Results of the Kruskal-Wallis analysis for circularity.

For the morphological shape parameters (aspect ratio and circularity), ANOVA cannot be used because the data are not normally distributed. Instead, we use the nonparametric Kruskal-Wallis test (https://www.mathworks.com/help/stats/kruskalwallis.html#btv4oqy-10) to check whether mineralogy is shape-dependent. For minerals with at least 30 observations, the Kruskal-Wallis test indicates that the circularities of different minerals are not statistically different (p-value = 0.054), and the effect size (in this case, ε^2) is negligible (ε^2 = 0.008). Likewise, the Kruskal-Wallis test results confirm that the aspect ratios of the mineral particles are not statistically different (p-value = 0.502, ε^2 = 0.004). These morphological results are visualized in Figs. 6b-c.

We also performed a principal component analysis (PCA) on the morphological and mineralogical data (see Text S2 in the Supplementary Materials) to assess the relationships between particle shape, size, and mineralogy. The results of the PCA are consistent with our observations from the ANOVA and Kruskal-Wallis tests. That is, the <5 µm dust deposited at Huascarán is well-sorted with respect to both morphology and mineralogy.

https://doi.org/10.5194/egusphere-2026-3846
Preprint. Discussion started: 8 July 2026

4.5 Temporal variability and trends

The previous sections considered the bulk morphological and mineralogical properties of dust preserved in HC-19A. However, information about temporal variability can also be inferred from the per-sample measurements for the 1960-2018 study period. The multiannual variability exhibited in the particle size (i.e., ECD), aspect ratio, and circularity data is presented in Fig. 7. While the quartile ranges for these measurements vary considerably from sample-to-sample, the time series for both shape metrics (aspect ratio and circularity) display consistent median values throughout the record. The median values for ECD are more variable. A pronounced local minimum in ECD is observed in the 2000-04 sample, implying that there was either an increase in dust emissions from distant source areas or a decrease in local dust emissions. The decrease in median ECD appears to have begun in 1995-99 and does not return to typical levels until 2010-14.

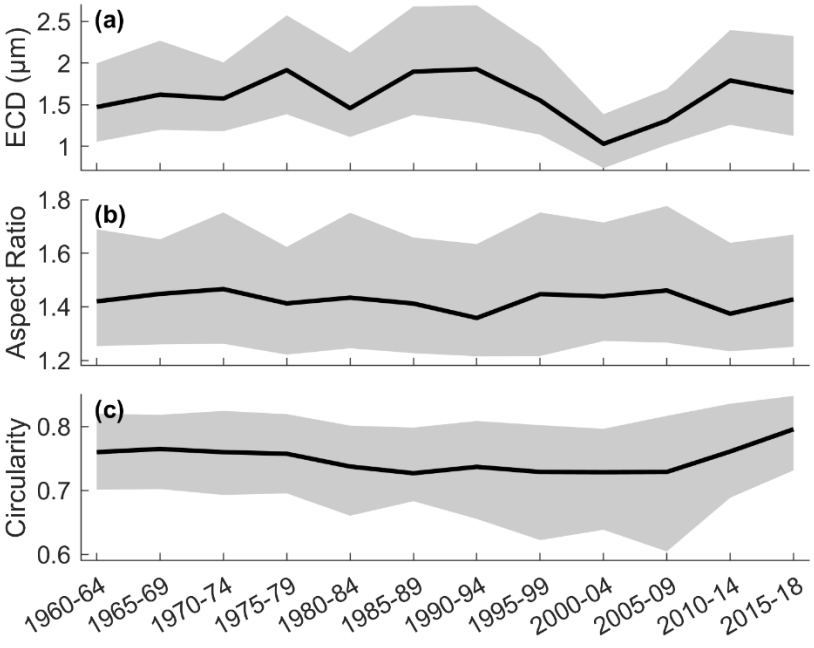

Figure 7. Time series of particle size and shape characteristics. Thick black lines represent median values; grey shaded areas show the 25%–75% quartile range. (a) Equivalent circular diameter. (b) Aspect ratio. (c) Circularity.

The multiannual variations in particle mineralogy are shown in Fig. 8. The stacked area plot in Fig. 8a confirms that minerals in the clay mineral group have consistently dominated the dust's overall composition since the start of the study period. Plagioclase, quartz, alkali feldspar, and mica constitute the other major mineral groups, albeit at much lower concentrations than the clay minerals.

https://doi.org/10.5194/egusphere-2026-3846
Preprint. Discussion started: 8 July 2026

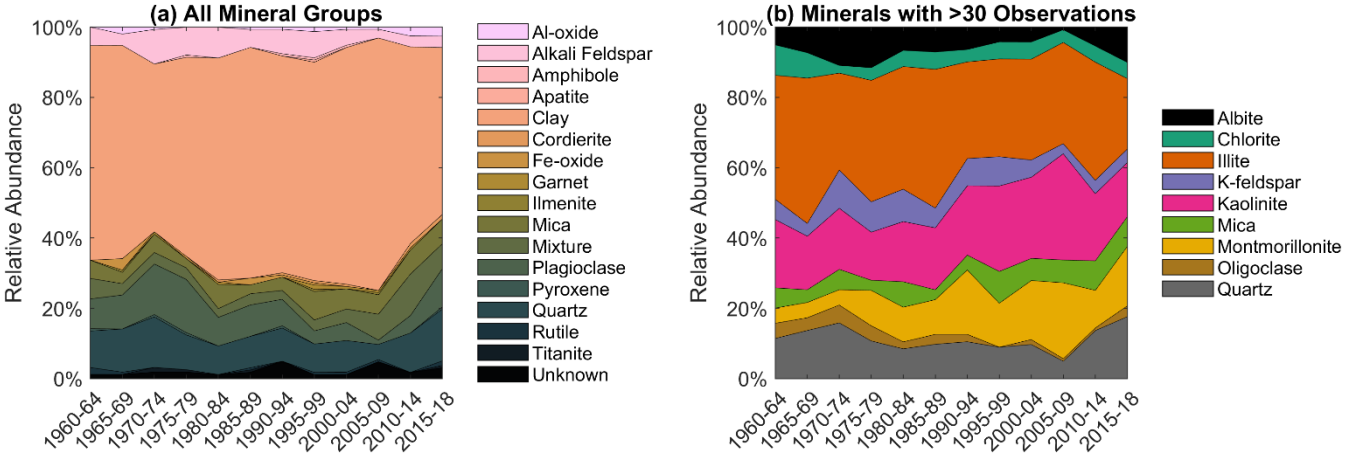

Figure 8. Stacked area time series plots showing relative mineral abundance. (a) All identified mineral groups. (b) Individual mineral species with at least 30 observations during the study period.

Moving forward in time starting from the 1995-99 sample, the general trends in the relative abundances of alkali feldspar, plagioclase, and quartz begin decreasing while the concentration of clay minerals increases. These trends peak in the 2005-09 sample. The inverse relationship between the former and latter mineral groups is most likely explained by the relative contributions of minerals from local and distal sources, respectively. Alkali feldspar, plagioclase, and quartz are the primary mineral assemblages found in the granodiorite bedrock of the Cordillera Blanca; in contrast, clay minerals (especially kaolinite) originate from more distant pedogenic (soil-borne) source areas. When dust contributions from one of these source regions are elevated, the relative abundance of dust originating in the other source region is thereby reduced in the ice core record.

The trends and patterns in the mineral group data are expanded upon in Fig. 8b, which focuses specifically on identified mineral species with at least 30 observations in the ice core record. The decrease (increase) in granodiorite (clay) minerals in the 2005-09 sample is apparent. The increase in clay minerals is largely driven by a change in the relative abundance of kaolinite—a clay mineral that is typically associated with the chemical weathering of soils in wet tropical environments (Schroeder and Erickson, 2014).

Another notable trend in the mineralogical data is a decrease in the abundance of clay minerals and a synchronous increase in quartz and plagioclase minerals between 2010 and 2018. This trend is indicative of a reduction in long-range transport and/or an increase in local dust emissions.

Finally, we note an interesting characteristic in the mineralogical data for the 1970-74 sample. Our SEM-EDS findings reveal that the relative abundance of granodiorite minerals (quartz, plagioclase, alkali feldspar) increased during this brief

https://doi.org/10.5194/egusphere-2026-3846
Preprint. Discussion started: 8 July 2026

period. This observation is noteworthy because the increase in the number of granodiorite minerals may be an artifact of the ill-famed 1970 Ancash earthquake. On 31 May 1970, a 7.9 moment magnitude earthquake dislodged 50–100 million m^3 of lithologic material from the northwest peak of Huascarán (Plafker et al., 1971). The resulting avalanche buried the villages of Yungay and Ranrahirca, killing thousands of people (Bode, 1989; Doughty, 1999; Plafker et al., 1971; Plafker and Ericksen, 1978). A "tremendous" cloud of dust is said to have descended down the mountain during the event (Plafker and Ericksen, 1978). Therefore, even though each dust filter represents a 5 y average, it is possible that this event left a mineralogical fingerprint in the dust records preserved on the Huascarán col.

5 Discussion

5.1 Potential drivers of the mineral dust signal

In the following sections, we discuss the potential sources of mineral dust deposited at Huascarán during the most recent six decades. We first consider the local dust signal—based on the presence of granodiorite-like minerals in the ice core record—which is related to the geology of the Cordillera Blanca and is likely affected by glacier retreat (Section 5.1.1). In Section 5.1.2 we speculate on the relationship between distally-sourced minerals (such as kaolinite) and forest cover changes in the Amazon Basin. Section 5.1.3 examines whether dust mineralogy may be related to aridity and dust storm events originating in North Africa. Other potential source areas are discussed in Section 5.1.4.

5.1.1 Glacier retreat

Glaciers can create dust sources via the erosion and deposition of fine glaciofluvial material or by exposing sediments during periods of glacier retreat or when snow cover is reduced (Bachelder et al., 2020; Bullard, 2013; Shugar et al., 2017; Xi et al., 2022). The Peruvian Cordillera Blanca has the highest concentration of tropical glaciers on Earth (Glas et al., 2018) and therefore the mountain range generates a substantial amount of proglacial sediments. This has likely been exacerbated by rapid glacier retreat in recent decades, the rates of which are considered unprecedented in the Holocene (Gorin et al., 2024). Since the Little Ice Age, the spatial extent of glaciers in the Cordillera Blanca has been reduced by half (Georges, 2004; Motschmann et al., 2020). Since the 1980s, the glaciers in the Cordillera Blanca have undergone a mass balance change of −38% (Yarleque, 2024). At Nevado Huascarán specifically, glaciers have diminished by 21% since 1987 (Schoessow, 2025). It remains possible that the retreat of these glaciers—and any resulting glaciofluvial sediment production or exposure—is contributing to local dust emissions. The subsequent aeolian transport and deposition of this dust back onto the glacier may then initiate a positive feedback that lowers the albedo of the surface snow, accelerates melting, and increases the availability of sediments for dust generation.

In a previous study, we (Weber et al., 2026a) simulated the impacts of dust on the col and summit of Huascarán using ice core microparticle size distribution records and the SNICAR radiative transfer model (Flanner et al., 2021). We found that at

https://doi.org/10.5194/egusphere-2026-3846
Preprint. Discussion started: 8 July 2026

these high-altitude sites (within the accumulation zone) dust has only a minimal impact on glacial albedo, but the magnitude of these effects may be greatly amplified at lower elevations. For instance, many of the glaciers at low elevations in the Cordillera Blanca are debris-covered (Mark et al., 2024). Previous investigations on the effective black carbon (eBC) contents of snow in the region have found that eBC concentrations are much higher at lower elevations and can significantly reduce surface albedo (Sánchez Rodríguez and Schmitt, 2018; Schmitt et al., 2015). Contributions of dust and other aeolian material as a result of glacier retreat may therefore pose a considerable threat.

The mineralogical characteristics of dust preserved in HC-19A show evidence of locally sourced material, albeit at much lower concentrations than the distally sourced clay minerals. There is some bias in this result, as our single particle analysis was primarily limited to the fraction of particles <5 µm in diameter. Larger particles (>10 µm) are inherently locally sourced due to their short atmospheric residence times, and thus the overall abundance of local dust is not considered within the scope of our investigation. Regardless, large dust particles are scarce in the Huascarán ice cores due to the extreme altitude of the drill site, which precludes efficient transport. Whatever large particles that do exist at Huascarán are necessarily sourced from the Cordillera Blanca, and, because of the third-power scaling of dust size as a function of particle diameter, the locally derived dust likely accounts for the bulk of the mineralogical material by volume. These particles are presumably consistent with the main granodiorite minerals identified in the Results section (i.e., quartz, plagioclase, and alkali feldspar), as well as biotite mica (another common mineral in granitic rocks) and muscovite from the phyllites of the Chicama Formation to the east.

However, the contribution of aeolian material from the Chicama Formation is less certain. One the one hand, a lack of observations of pyrite in the dust filters may indicate that the Chicama Formation is a negligible source of local dust. Pyrite is common in the Chicama Formation (Atherton and Sanderson, 1987), and sulfide leaching from these minerals is directly related to downstream water contamination (Fortner et al., 2011; Glas et al., 2018; Magnússon et al., 2020). On the other hand, the absence of pyrite in the dust filter samples may simply be a consequence of pyrite's high density (4.8–5.0 g cm^3), which greatly increases its settling velocity as an aerosol. Muscovite, in contrast, is morphologically ideal for transport to the ice core site because of its erodibility, low density (2.8–2.9 g cm^3), and sheet-like crystal habit, which increases the particles' drag coefficient (Reid et al., 2003; Wiese et al., 2015). In a mineral dust assessment of a firn core from Nevado Illimani (Bolivia), Lindau et al. (2021) show that phyllosilicates such as muscovite/illite have prolonged atmospheric residence times and are preferentially removed by wet deposition and that the suspension of very large dust grains (>20 µm) is facilitated by strong downdrafts related to deep convection. More work needs to be done to quantify the amount of dust generated within the Cordillera Blanca, as well as the mechanisms of uplift of these particles towards the summits—particularly with respect to glacier retreat—but the presence of granodiorite minerals and muscovite in the ice core record is reasonably attributable to local origins.

https://doi.org/10.5194/egusphere-2026-3846
Preprint. Discussion started: 8 July 2026

5.1.2 Forest cover change

Natural and anthropogenic vegetation changes within the Amazon are another potential driver of the dust record preserved in the Huascarán ice. The disturbance of soils due to urbanization, agricultural and farmland expansion, and deforestation likely increases the amount of dust emitted from the Amazon, as supported by observational and model evidence from various parts of the world (Betts et al., 2008; Engelbrecht and Derbyshire, 2010; Ginoux et al., 2012; Kok et al., 2023; Stanelle et al., 2014; Tegen et al., 1996; Tegen and Fung, 1995). Global dust mass loading has increased by 55 ± 30% since the pre-Industrial era, with approximately 33% of this increase due to human land use (Kok et al., 2023).

Since the 1970s, there has been considerable disturbance of forests in the Amazon (Fearnside, 2005; Kalamandeen et al., 2018; Malhi et al., 2008; Nobre et al., 1991; Silva Junior et al., 2021), with recent estimates suggesting that 38% of the Amazon has been disturbed by human activity while 17% has been deforested (Albert et al., 2023; Harvey, 2023; Lapola et al., 2023). Beyond 20–25% deforestation, the Amazon is expected to surpass an irreversible tipping point that will flip eastern, southern, and central Amazonia toward non-forest ecosystems (Lovejoy and Nobre, 2018). The effects of land use change in the Amazon may also be leading to precipitation reductions (Baudena et al., 2021; Leite-Filho et al., 2021; Mu and Jones, 2022) and intensified droughts (Staal et al., 2020).

Deforestation rates have varied considerably both spatially and temporally over the last few decades. For example, deforestation rates in the Brazilian Amazon peaked in 2004 (at nearly 28,000 km^2 y^{-1}) before the adoption of an action plan that led to an 84% reduction in deforestation rates by 2012 (Silva Junior et al., 2021). However, there has been an uptick in deforestation rates since 2013, with 11,000 km^2 of forest loss in 2020 (Silva Junior et al., 2021). In Peru, the deforestation rate from 2001 to 2016 was higher than the rate from 1987 to 2001 (Rojas Briceño et al., 2019). In addition, the rate of deforestation in Peru spiked during the COVID-19 pandemic (Céspedes et al., 2023). The main drivers of deforestation in Peru are agricultural expansion and the development of transport infrastructure (Rojas Briceño et al., 2019), but deforestation due to gold mining is also common (Caballero Espejo et al., 2018; Diringer et al., 2020). Bourgeois et al. (2015) showed that aerosols emitted over the Amazon Basin can be transported westward and lifted along the eastern slopes of the Andes, reaching the free troposphere at elevations comparable to tropical glacier summits.

Any dust emissions related to the degradation of forests in the Amazon will be compositionally linked to soil mineralogy. In the Amazon lowlands, soils are dominated by the clay mineral kaolinite (in many cases by more than 80%), although the formation of montmorillonite is favoured in areas of poor drainage (Irion, 1984). In the western parts of the basin, illite clays are common in addition to kaolinite and oxide minerals (Guyot et al., 2007).

https://doi.org/10.5194/egusphere-2026-3846
Preprint. Discussion started: 8 July 2026

Given the abundance of kaolinite in the Amazon and the relationship between deforestation and dust emissions, it is possible that the kaolinite contents in the Huascarán ice cores may be interpreted as a proxy of forest cover change. Indeed, the positive trend observed in the ice core kaolinite record from the early 1990s through the present appears to reflect deforestation rates in the Brazilian Amazon (Fig. 9). Kaolinite concentrations peak in the 2005-09 sample, just after the 2004 peak in deforestation rates. Following the peak is a corresponding decrease in both deforestation rate and kaolinite concentrations. Unfortunately, due the multiannual (5 y) resolution of our mineralogical measurements and the short temporal overlap (1985–2018, n=7), we cannot draw any statistical conclusions about the correlation between the rate of forest loss and kaolinite at Huascarán; however, consistency between the trends demonstrates the plausibility of a mechanistic relationship.

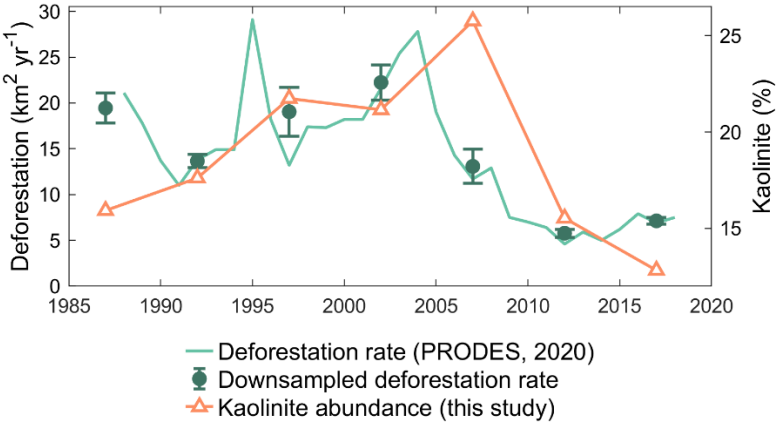

Figure 9. Deforestation rates and ice core kaolinite abundance. Official deforestation rates (green) for the Brazilian Legal Amazon (PRODES, 2020). The down-sampled deforestation rates include standard error bars. Kaolinite abundance in HC-19A (orange) exhibits similar trends to the annual deforestation record with a 2−3 y lag.

5.1.3 African aridity

A third potential source of dust to Huascarán is North Africa, although the distance between the two sites is quite immense (e.g., it is approximately 7,400 km from Huascarán to the west coast of Mauritania). Despite the extremity of the transport pathway, such long-range distances are not impossible (Van Der Does et al., 2018). In fact, the lateral movement of African dust towards the eastern Amazon during the austral summer is a well-documented phenomenon (Abouchami et al., 2013; Besl, 2022; Bristow et al., 2010; Koren et al., 2006; Prospero et al., 1981, 2020, 2021; Yu et al., 2015, 2020).

Whether African dust makes its way across the Amazon toward the Andes is comparatively understudied. Marine sediment records from the eastern equatorial Pacific show evidence of varying amounts of African-sourced dust on millennial time scales (Schimmenti et al., 2025). This finding suggests that African dust is capable of being transported across tropical South

https://doi.org/10.5194/egusphere-2026-3846
Preprint. Discussion started: 8 July 2026

America and over the Andes. MERRA-2 satellite products have also been used to show that African dust can be deposited over central Colombia (Prospero et al., 2020). Similarly, Bolaño-Ortiz et al. (2023) used remote sensing data from MERRA-2 and MODIS to correlate snow albedo changes in the Colombian Andes with Saharan dust outbreaks. Likewise, Boy and Wilcke (2008) found evidence of African dust deposited in the Ecuadorian Andes. In addition, Davis (2002) identified a correlation between the concentrations of microparticles at Huascarán and surface level pressures over central Africa from 1949 to 1992, although it should be noted that first-order trends within the data likely drive the correlations. A more thorough statistical investigation with detrending analysis was not conducted. It remains to be studied—either through the lens of mineralogical evidence or geochemical evidence—whether sufficient quantities of African dust are transported to the Cordillera Blanca. Prospero et al. (2020), for example, note that even though African dust can reach Colombia, the dust concentrations are about one-fifth of the concentrations observed at Cayenne on the Atlantic coast of French Guiana. Most of the dust is conceivably removed from the atmosphere during transport across the Amazon by rainout effects.

The aridification of global dust hotspots since the 1960s is noted by Sardans et al. (2024), which includes North Brazil, North Africa, the Middle East, and the Sahel. Trade wind intensification and surface level pressure trends in tropical latitudes have also been observed in recent decades (McGregor et al., 2018). Moreover, Dolce and Miller (2025) find that the frequency of African dust events has increased over the last four decades. Such trends may be responsible for the increasing dust concentrations observed in the Huascarán ice cores (Weber et al., 2026a). However, results from a recent study by Yeo et al. (2026) show no evidence of increased dust activity in the Sahara or the Sahel since the 1980s. In fact, the authors find that dust emissions in North Africa are related to the large-scale Atlantic Multidecadal Oscillation (AMO), indicating that the frequency of North African dust storms may continue to decline under future warming and AMO phases.

The mineralogical composition of African dust is highly heterogeneous depending on the exact source region (e.g., Caquineau et al., 1998; Engelbrecht and Derbyshire, 2010; Moreno et al., 2006; Mounkaila, 2006; Muhs et al., 2014; Scheuvens et al., 2013). The Bodélé depression in central Africa, for instance, emits more than 0.7 million tons of dust per day and was once thought to be the greatest source of dust to the Amazon Basin (Koren et al., 2006). However, x-ray diffraction analyses of soil samples in the region reveal that mineralogy varies considerably by latitude, with high kaolinite concentrations dominating the clay mineral fraction in the north while montmorillonite is more prevalent in the south (Mounkaila, 2006). The Bodélé depression is unlikely to be a primary driver of the Huascarán dust signal, however, as recent studies have found that the El Djouf region in northwest Africa is the preferred source for the transatlantic flux of dust to South America (Yu et al., 2020).

Panta et al. (2023) analyzed more than 300,000 airborne mineral particles from the Moroccan Sahara and found that illite (27%) and kaolinite (16%) are the main species in the 1–2 μm fraction. Dust deposits in the Canary Islands have a similar concentration of illite (26%) but a lower kaolinite content (5%) (Menéndez et al., 2014). However, perhaps the most

https://doi.org/10.5194/egusphere-2026-3846
Preprint. Discussion started: 8 July 2026

significant mineralogical characteristic of dust from Africa is the presence of the clay mineral palygorskite. While typically only found in low abundance (e.g., Nowak et al. (2018) found that soil samples from Tunisia contain less than 6% palygorskite), palygorskite is commonly used as a source tracer in dust analyses because it can be found in African soils (Avila et al., 1997; Caquineau et al., 1998, 2002; Ganor, 1991; Menéndez et al., 2007; Moreno et al., 2006; Rodriguez-Navarro et al., 2018; Rostási et al., 2022; Scheuvens et al., 2013; Tomadin and Lenaz, 1989). None of the 1887 identified mineral particles in HC-19A exhibited elemental spectra consistent with palygorskite, despite notable trans-Atlantic African dust events occurring during the study period (e.g., Evan and Mukhopadhyay, 2010; Petit et al., 2005). The procedure used to classify mineral particles in this study included a machine learning algorithm trained to recognize palygorskite, thus the lack of this clay mineral in our samples is unlikely to be due to limitations in our methodology. This finding should draw into question whether North Africa can be inferred as a significant source of dust to Huascarán.

5.1.4 Other potential sources

There are other dust sources that may contribute to what is archived at Huascarán, however we deem these sources less likely than the ones described above. Such sources include the high Puna-Altiplano deserts, with frequent dust storms originating in the Salar de Uyuni (southern Altiplano, Bolivia) and in the Salinas Grandes (northern Puna, Argentina) throughout the year (Gaiero et al., 2013). Due to their geographical positions relative to the trade wind direction and the South American Low-Level Jet (SALLJ), the dominant transport direction from these sources is toward the southeast. The Bolivian dust source areas are south and southeast of Huascarán and are subjected to the atmospheric currents of the SALLJ, which moves from north to south along the eastern flank of the tropical Andes (Montini et al., 2019). However, it was shown that some winter circulation patterns may allow dust transport toward Peru (Olmo et al., 2022), particularly considering that plumes can reach elevations up to 8000 m a.s.l. (Gaiero et al., 2013).

Another potential source is coastal Peru, where 4–5 dust storms per year have been documented (Briceño-Zuluaga et al., 2017). The coastal desert is located west of the Cordillera Blanca and, in consequence, the easterly trade winds generally blow dust at the surface away from Huascarán rather than towards it. There is currently no direct evidence that dust plumes from specific coastal dust storms reach the Cordillera Blanca, however meteorological analyses indicate upslope and cross-valley winds from the Pacific coast toward the highest peaks of the Cordillera Blanca (Rosales et al., 2022), which could potentially entrain and transport particles from arid coastal regions located ~100 km away.

In both cases, atmospheric mixing and differences in the circulation patterns at upper levels could still carry some of this dust (including some specific deposition events) to the ice core site—but probably not as frequently or in great enough quantities to be a primary source of mineral dust to Huascarán on annual timescales.

https://doi.org/10.5194/egusphere-2026-3846
Preprint. Discussion started: 8 July 2026

5.2 Mineral ratios

Oftentimes, dust studies compare isotopic measurements (e.g., Sr/Nd or Pb isotope ratios), trace element chemistry data, and/or rare earth element chemistry data with reference data obtained from potential source area (PSA) samples. Such techniques are a powerful means of "fingerprinting" the origins of dust (Beaudon et al., 2022; Sierra-Hernández et al., 2024; Svensson et al., 2000). In our case, we are working with measurements acquired with SEM-EDS. Unfortunately, the trace element detection capabilities of EDS are inferior to more powerful techniques such as wavelength dispersive spectrometry (Lavrent'ev et al., 2015), and so it is not possible to study dust provenance from a geochemical perspective using the data in this study. Instead, we must rely on the relative abundances of individual mineral groups to infer the origins of the particles.

The ratios of clay mineral species are frequently used as a metric for comparison with PSAs. For instance, the ratio of kaolinite to chlorite (K/C) can be used as a proxy for distinguishing between low- and high-latitude dust sources (Biscaye, 1965; Biscaye et al., 1997; Bory et al., 2002; Donarummo et al., 2003; Maggi, 1997; Nagatsuka et al., 2021). The latitudinal variability of K/C ratios is due to differences in weathering regimes, with high chemical weathering in low latitudes favouring the production of kaolinite while a shift toward mechanical weathering at higher latitudes favours the production of chlorite (Biscaye et al., 1997). Bory et al. (2002) show that low-latitude K/C ratios typically fall between 1 and 10. The dust samples from HC-19A are consistent with this finding, as we calculate a K/C ratio of 4.1 based on the observation of 325 kaolinite particles and 80 chlorite particles across the full study period.

Another commonly used mineral ratio is illite/kaolinite (I/K). Caquineau et al. (1998) were the first to show that I/K ratios can be used as a dust provenance tracer. The authors compared the I/K ratios of Saharan-derived dust over Cape Verde to dust carried westward to the Caribbean Sea and found that I/K ratios do not fractionate during long-range transport. I/K ratios have since been applied to dust studies from many regions of the world to determine the origins of dust through the lens of mineralogy (e.g., Scheuvens et al., 2013 and references therein).

The I/K ratio for HC-19A across the full study period is 1.6 and is shown in Fig. 10 along with violin plots comparing the variability of I/K ratios in HC-19A with I/K ratios for the Amazon (Guyot et al., 2007) and North Africa (Caquineau et al., 1998, 2002). There is notable agreement between the I/K ratios observed in HC-19A and the I/K ratios in the western Amazon (Fig. 10a), as well as moderate agreement with I/K ratios in the central Amazon (Fig. 10b) and weak agreement with I/K ratios in the eastern Amazon (Fig. 10c). This finding is consistent with a regional dust source within the Amazon Basin, with a greater likelihood moving westward towards the tropical Andes.

However, there is also a very strong agreement between the I/K ratios in HC-19A and the I/K ratios observed in the northwestern Sahara (Fig. 10d). There is no consistency between the ice core I/K ratio record and the I/K ratios observed in

https://doi.org/10.5194/egusphere-2026-3846
Preprint. Discussion started: 8 July 2026

the central Sahara (Fig. 10e) or the African Sahel (Fig. 10f). This finding may support the conclusions of Yu et al. (2020) who argue that the El Djouf region in northwestern Africa is the dominant source of dust transported to the Amazon Basin (as opposed to the Bodélé depression in central Africa). However, this finding is complicated by overlapping consistency with I/K ratios found in Amazonian soils.

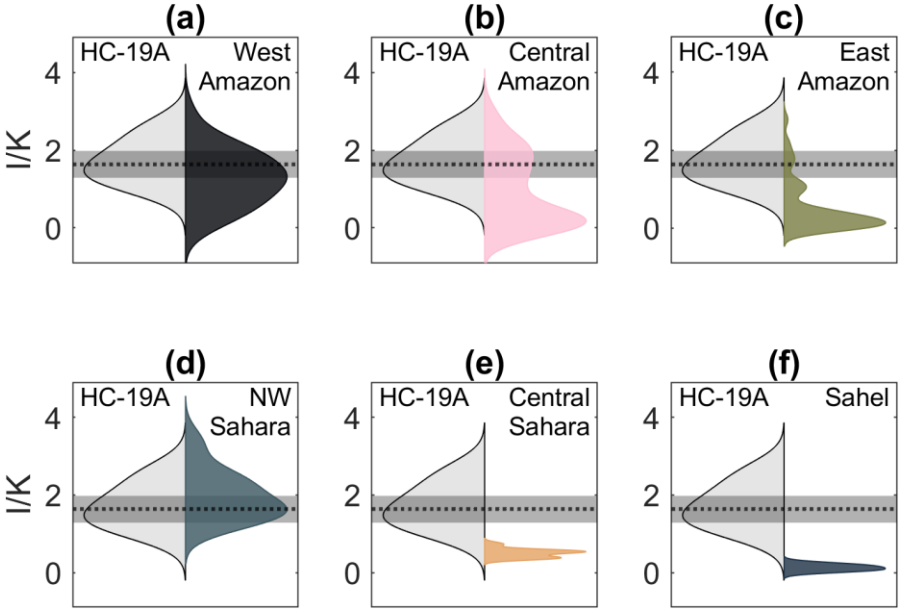

Figure 10. Violin plots comparing illite/kaolinite (I/K) ratios in HC-19A to potential source areas. In all figures, the black dotted line represents the calculated I/K ratio across all samples, and the surrounding shaded area is the 3σ (~99%) confidence interval based on Poisson uncertainty. The shapes of the violin plots illustrate kernel density estimates based on the I/K ratios of each sample. The I/K ratios of HC-19A are shown on the lefthand side of each violin plot. The I/K ratios of the PSAs are shown on the righthand side of each violin plot. (a-c) Soil mineral data are from Guyot et al. (2007). The Amazon is divided into three sub-regions: West (west of 65°W); Central (between 70°W and 60°W); and East (east of 65°W). In addition, all Amazonian sub-regions correspond to latitudes north of 12°S. (d-f) Soil mineral data are from Caquineau et al. (1998, 2002).

It is apparent that for our study site mineralogical ratios are an ambiguous indicator of dust source. There is perhaps more overall consistency with Amazonian soils, and the lack of observations of palygorskite in HC-19A lends support to the Amazonian hypothesis, but the consistency with I/K ratios in the northwestern Sahara means that Africa cannot be ruled out as a primary source of long-range dust to Huascarán. Further analyses that employ geochemical or isotopic PSA fingerprinting will be vital to fully unravelling the mystery behind the origins of the clay minerals deposited at the ice core site.

https://doi.org/10.5194/egusphere-2026-3846
Preprint. Discussion started: 8 July 2026

5.3 HYSPLIT trajectory simulations

To contextualize our discussion of potential dust sources, we show air mass trajectory frequency maps for the early wet season (DJF), late wet season (MAM), and dry season (JJAS) derived from HYSPLIT model simulations (Fig. 11). During the wet season months, air masses originating from Africa near the surface level move toward tropical South America while the air masses 6000 m a.s.l. arriving at Huascarán may intercept dust from these regions. In contrast, during the dry season, upper-level backward trajectories at Huascarán most frequently originate within the Andes and to the northwest. The transport of dust from Africa to Huascarán during the dry season is not supported by our HYSPLIT simulations.

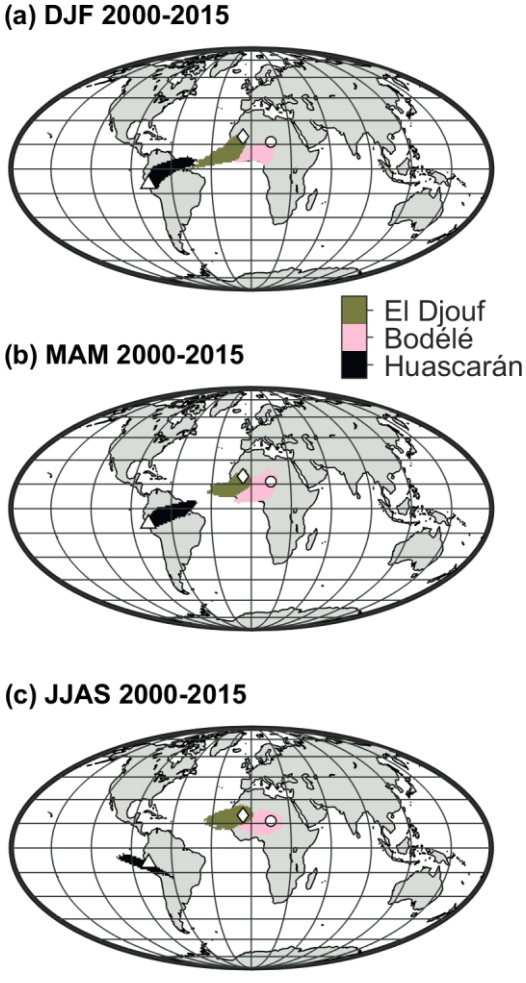

Figure 11. HYSPLIT 10 d ensemble trajectory frequency models. (a) Early wet season months December–February 2000–2015. (b) Late wet season months March–May 2000–2015. (c) Dry season months June–September 2000-2015. The El Djouf (diamond, green) and Bodélé (circle, pink) trajectories represent forward simulations pinpointing where at least 2.5%

https://doi.org/10.5194/egusphere-2026-3846
Preprint. Discussion started: 8 July 2026

of trajectories passed through; the Huascarán (triangle, black) trajectories represent backward simulations showing where at least 5% of the trajectories passed through, pinpointing only the regions with the highest frequency airflow.

The trajectory frequency analysis suggests that the Peruvian coastal desert and the Bolivian Altiplano should not be discounted as potential dust source areas. However, it is difficult to describe a realistic mechanism by which dust from these regions may be deposited at the ice core site. The climatology of the SALLJ and 850 hPa winds theoretically should divert surface-level dust from these source areas away from Huascarán (e.g., Montini et al., 2019), but it is not possible to use our two-dimensional HYSPLIT simulations to interpret the effects of vertical motion. A more detailed modelling study is needed to understand how dry season dust emissions from coastal Peru and the Altiplano could reach Huascarán. In addition, it is difficult to reconcile how dust is incorporated into the snowpack at Huascarán during the dry season without a wet deposition mechanism. That is, the severe lack of precipitation events in the Cordillera Blanca during the dry season (Vuille et al., 2008) substantially limits the settling of particles by wet deposition. Gravitational settling by dry deposition is therefore the dominant factor by which dust reaches the glacial surfaces on the Huascarán col during JJAS. However, the funnelling of air between the mountain peaks greatly enhances wind speeds on the col and likely prevents significant amounts of dust from accumulating. In addition, the dry conditions at Huascarán from June through September augment the glacial ablation rate, which concentrates dust that accumulated during the previous wet season months (Davis, 2002). For this reason, the dry season dust signal preserved at Huascarán is likely related to dust deposition that occurred during the wet season. Our interpretations of the mineralogical data are primarily grounded from this perspective; however, we note that more work is needed to definitively understand the seasonality of dust at Huascarán.

6 Conclusions

To our knowledge, this study is the first to use an ice core to characterize the morphology and composition of mineral dust in the tropical Andes. We used a scanning electron microscope with energy dispersive x-ray spectrometry (SEM-EDS) to analyze 1887 fine-grain (<5 μm diameter) mineral particles in the 2019 Huascarán Col A ice core (HC-19A) for size distributions, circularity, aspect ratio, and mineralogy.

The mineral dust particles are lognormally distributed by equivalent circular diameter and exhibit a median circularity of 0.75 ± 0.01 (std. error) and a median aspect ratio of 1.42 ± 0.03 (std. error). The most common minerals observed in the EDS data belong to the clay mineral group (e.g., illite, kaolinite, and montmorillonite), accounting for 60% of the total dust count. There is little evidence of size- or shape-dependency for the mineral grains, and the overall composition of the dust has been relatively stable across the most recent six decades. Slight trends in the morphological data and the mineralogical data may be used as evidence for reconstructing environmental changes or shifts in atmospheric circulation patterns. For instance, particle sizes are lowest in the dust sample for 2000-2004, which may indicate an increase in transport from distal source

https://doi.org/10.5194/egusphere-2026-3846
Preprint. Discussion started: 8 July 2026

areas and/or a decrease in local dust emissions. Similarly, an increase in the relative abundance of kaolinite during the mid-2000s correlates with forest cover changes in the Amazon and may be mechanistically linked to enhanced dust emissions due to deforestation.

More work is needed to definitively trace the origins of the dust preserved at Huascarán. Such analyses may include Sr/Nd isotope fingerprinting or complex atmospheric transport modelling. In any case, the data set reported here is highly unique and has the potential to enhance our understanding of the dynamics of mineral dust in tropical South America and the Peruvian Andes in particular.

Code and data availability

The ice core data are available through the NOAA National Centers for Environmental Information World Data Service for Paleoclimatology here: https://doi.org/10.25921/1j1e-tf69 (Weber et al., 2026b). A compiled document of the MATLAB® code used in this study is available on Zenodo here: https://doi.org/10.5281/zenodo.20817171 (Weber, 2026).

Supplement link

The link to the supplement will be included by Copernicus, if applicable.

Author contributions

AMW was responsible for the conceptualization of the study, formal analysis, funding acquisition (FOH), software, visualization, and writing (original draft). LGT was responsible for funding acquisition (NSF), project administration, and supervision. AMW, SK, EB, MRSH, LHB, and DK contributed to investigation. AMW, MD, and LGT contributed to data curation. AMW, LHB, and DK contributed to the methodology. AMW, SK, and LHB contributed to validation. All authors contributed to writing (review & editing).

Competing interests

The authors declare that they have no conflict of interest.

Disclaimer

Copernicus Publications adds a standard disclaimer: “Copernicus Publications remains neutral with regard to jurisdictional claims made in the text, published maps, institutional affiliations, or any other geographical representation in this paper.

https://doi.org/10.5194/egusphere-2026-3846
Preprint. Discussion started: 8 July 2026

While Copernicus Publications makes every effort to include appropriate place names, the final responsibility lies with the authors. Views expressed in the text are those of the authors and do not necessarily reflect the views of the publisher."
Please feel free to add disclaimer text at your choice, if applicable.

695 **Acknowledgements**

This research was made possible by the efforts of the 2019 Huascarán field team for recovering the ice core used in this study. We thank Friends of Orton Hall for funding our electron microscopy research, which was performed at the Center for Electron Microscopy and Analysis (CEMAS) at The Ohio State University. This material is based upon work supported by the National Science Foundation under Award No. 1805819. Any opinions, findings and conclusions or recommendations
700 expressed in this material are those of the authors and do not necessarily reflect the views of the National Science Foundation. This is Byrd Polar and Climate Research Center contribution No. C-1644.

Financial support

The electron microscopy was supported by Friends of Orton Hall (FOH). The 2019 ice core recovery was supported by the National Science Foundation (NSF) under Award No. 1805819.

705 **Review statement**

The review statement will be added by Copernicus Publications listing the handling editor as well as all contributing referees according to their status anonymous or identified.

References

Abouchami, W., Näthe, K., Kumar, A., Galer, S. J. G., Jochum, K. P., Williams, E., Horbe, A. M. C., Rosa, J. W. C.,
710 Balsam, W., Adams, D., Mezger, K., and Andreae, M. O.: Geochemical and isotopic characterization of the Bodélé Depression dust source and implications for transatlantic dust transport to the Amazon Basin, Earth Planet. Sci. Lett., 380, 112–123, https://doi.org/10.1016/j.epsl.2013.08.028, 2013.

Albert, J. S., Carnaval, A. C., Flantua, S. G. A., Lohmann, L. G., Ribas, C. C., Riff, D., Carrillo, J. D., Fan, Y., Figueiredo, J. J. P., Guayasamin, J. M., Hoorn, C., De Melo, G. H., Nascimento, N., Quesada, C. A., Ulloa Ulloa, C., Val, P., Arieira, J.,
715 Encalada, A. C., and Nobre, C. A.: Human impacts outpace natural processes in the Amazon, Science, 379, eabo5003, https://doi.org/10.1126/science.abo5003, 2023.

Allison, E. A.: The spiritual significance of glaciers in an age of climate change, WIREs Clim. Change, 6, 493–508, https://doi.org/10.1002/wcc.354, 2015.

https://doi.org/10.5194/egusphere-2026-3846
Preprint. Discussion started: 8 July 2026

Atherton, M. P. and Petford, N.: Generation of sodium-rich magmas from newly underplated basaltic crust, Nature, 362, 144–146, https://doi.org/10.1038/362144a0, 1993.

Atherton, M. P. and Sanderson, L. M.: The Cordillera Blanca Batholith: A study of granite intrusion and the relation of crustal thickening to peraluminosity, Geol. Rundsch., 76, 213–232, https://doi.org/https://doi.org/10.1007/BF01820584, 1987.

Avila, A., Queralt-Mitjans, I., and Alarcón, M.: Mineralogical composition of African dust delivered by red rains over northeastern Spain, J. Geophys. Res.: Atmos., 102, 21977–21996, https://doi.org/10.1029/97JD00485, 1997.

Bachelder, J., Cadieux, M., Liu-Kang, C., Lambert, P., Filoche, A., Galhardi, J. A., Hadioui, M., Chaput, A., Bastien-Thibault, M.-P., Wilkinson, K. J., King, J., and Hayes, P. L.: Chemical and microphysical properties of wind-blown dust near an actively retreating glacier in Yukon, Canada, Aerosol Sci. Technol., 54, 2–20, https://doi.org/10.1080/02786826.2019.1676394, 2020.

Baudena, M., Tuinenburg, O. A., Ferdinand, P. A., and Staal, A.: Effects of land-use change in the Amazon on precipitation are likely underestimated, Global Change Biol., 27, 5580–5587, https://doi.org/10.1111/gcb.15810, 2021.

Beaudon, E., Sheets, J. M., Martin, E., Sierra-Hernández, M. R., Mosley-Thompson, E., and Thompson, L. G.: Aeolian Dust Preserved in the Guliya Ice Cap (Northwestern Tibet): A Promising Paleo-Environmental Messenger, Geosciences, 12, 366, https://doi.org/10.3390/geosciences12100366, 2022.

Besl, J.: Africa's earth, wind, and fire keep the Amazon green, Eos, 103, 22–29, https://doi.org/https://doi.org/10.1029/2022EO220151, 2022.

Betts, R., Sanderson, M., and Woodward, S.: Effects of large-scale Amazon forest degradation on climate and air quality through fluxes of carbon dioxide, water, energy, mineral dust and isoprene, Phil. Trans. R. Soc. B, 363, 1873–1880, https://doi.org/10.1098/rstb.2007.0027, 2008.

Biscaye, P. E.: Mineralogy and Sedimentation of Recent Deep-Sea Clay in the Atlantic Ocean and Adjacent Seas and Oceans, Geol. Soc. Am. Bull., 76, 803--832, 1965.

Biscaye, P. E., Grousset, F. E., Revel, M., Van der Gaast, S., Zielinski, G. A., Vaars, A., and Kukla, G.: Asian provenance of glacial dust (stage 2) in the Greenland Ice Sheet Project 2 Ice Core, Summit, Greenland, J. Geophys. Res.: Oceans, 102, 26765–26781, https://doi.org/10.1029/97JC01249, 1997.

Blifford, I. H. and Gillette, D. A.: Applications of the lognormal frequency distribution to the chemical composition and size distribution of naturally occurring atmospheric aerosols, Water Air Soil Pollut., 1, 106–114, https://doi.org/10.1007/BF00280783, 1971.

Bode, B.: No Bells to Toll: Destruction and Creation in the Andes, Paragon House, New York, NY, 559 pp., 1989.

Bolaño-Ortiz, T., Diaz Gutierrez, V., Vélez-Pereira, A., Vergara, E., and Camargo Caicedo, Y.: Snow Albedo Reduction in the Colombian Andes Mountains Due to 2000 to 2020 Saharan Dust Intrusions Events, Water, 15, https://doi.org/10.3390/w15173150, 2023.

Bory, A. J.-M., Biscaye, P. E., Svensson, A., and Grousset, F. E.: Seasonal variability in the origin of recent atmospheric mineral dust at NorthGRIP, Greenland, Earth Planet. Sci. Lett., 196, 123–134, https://doi.org/10.1016/S0012-821X(01)00609-4, 2002.

https://doi.org/10.5194/egusphere-2026-3846
Preprint. Discussion started: 8 July 2026

Bourgeois, Q., Ekman, A. M. L., and Krejci, R.: Aerosol transport over the Andes from the Amazon Basin to the remote Pacific Ocean: A multiyear CALIOP assessment, J. Geophys. Res.: Atmos., 120, 8411–8425, https://doi.org/10.1002/2015JD023254, 2015.

Boy, J. and Wilcke, W.: Tropical Andean forest derives calcium and magnesium from Saharan dust, Global Biogeochem. Cycles, 22, https://doi.org/10.1029/2007GB002960, 2008.

Briceño-Zuluaga, F., Castagna, A., Rutllant, J. A., Flores-Aqueveque, V., Caquineau, S., Sifeddine, A., Velazco, F., Gutierrez, D., and Cardich, J.: Paracas dust storms: Sources, trajectories and associated meteorological conditions, Atmos. Environ., 165, 99–110, https://doi.org/10.1016/j.atmosenv.2017.06.019, 2017.

Bristow, C. S., Hudson-Edwards, K. A., and Chappell, A.: Fertilizing the Amazon and equatorial Atlantic with West African dust, Geophys. Res. Lett., 37, L14807, https://doi.org/10.1029/2010GL043486, 2010.

Bullard, J. E.: Contemporary glacigenic inputs to the dust cycle, Earth Surf. Processes Landforms, 38, 71–89, https://doi.org/10.1002/esp.3315, 2013.

Bullock, E. L., Woodcock, C. E., Souza Jr., C., and Olofsson, P.: Satellite-based estimates reveal widespread forest degradation in the Amazon, Global Change Biol., 26, 2956–2969, https://doi.org/10.1111/gcb.15029, 2020.

Buseck, P. R.: Atmospheric-particle research: Past, present, and future, Elements, 6, 208–209, 2010.

Caballero Espejo, J., Messinger, M., Román-Dañobeytia, F., Ascorra, C., Fernandez, L. E., and Silman, M.: Deforestation and Forest Degradation Due to Gold Mining in the Peruvian Amazon: A 34-Year Perspective, Remote Sens., 10, 1903, https://doi.org/10.3390/rs10121903, 2018.

Caquineau, S., Gaudichet, A., Gomes, L., Magonthier, M.-C., and Chatenet, B.: Saharan dust: Clay ratio as a relevant tracer to assess the origin of soil-derived aerosols, Geophys. Res. Lett., 25, 983–986, https://doi.org/10.1029/98GL00569, 1998.

Caquineau, S., Gaudichet, A., Gomes, L., and Legrand, M.: Mineralogy of Saharan dust transported over northwestern tropical Atlantic Ocean in relation to source regions, J. Geophys. Res., 107, https://doi.org/10.1029/2000JD000247, 2002.

Carey, M.: Living and dying with glaciers: people's historical vulnerability to avalanches and outburst floods in Peru, Global Planet. Change, 47, 122–134, https://doi.org/10.1016/j.gloplacha.2004.10.007, 2005.

Carrivick, J. L. and Tweed, F. S.: A global assessment of the societal impacts of glacier outburst floods, Global Planet. Change, 144, 1–16, https://doi.org/10.1016/j.gloplacha.2016.07.001, 2016.

Céspedes, J., Sylvester, J. M., Pérez-Marulanda, L., Paz-Garcia, P., Reymondin, L., Khodadadi, M., Tello, J. J., and Castro-Nunez, A.: Has global deforestation accelerated due to the COVID-19 pandemic?, J. For. Res., 34, 1153–1165, https://doi.org/10.1007/s11676-022-01561-7, 2023.

Chevallier, P., Pouyaud, B., Suarez, W., and Condom, T.: Climate change threats to environment in the tropical Andes: glaciers and water resources, Reg. Environ. Change, 11, 179–187, https://doi.org/10.1007/s10113-010-0177-6, 2011.

Dang, C., Brandt, R. E., and Warren, S. G.: Parameterizations for narrowband and broadband albedo of pure snow and snow containing mineral dust and black carbon, J. Geophys. Res.: Atmos., 120, 5446–5468, https://doi.org/10.1002/2014JD022646, 2015.

https://doi.org/10.5194/egusphere-2026-3846
Preprint. Discussion started: 8 July 2026

Davis, M. E.: Climatic interpretations of eolian dust records from low-latitude, high-altitude ice cores, Ph.D. thesis, The Ohio State University, USA, 365 pp., http://rave.ohiolink.edu/etdc/view?acc_num=osu1486461246816301, 2002.

Di Mauro, B., Garzonio, R., Ravasio, C., Orlandi, V., Baccolo, G., Gilardoni, S., Remias, D., Leoni, B., Rossini, M., and Colombo, R.: Combined effect of algae and dust on snow spectral and broadband albedo, J. Quant. Spectrosc. Radiat. Transfer, 316, 108906, https://doi.org/10.1016/j.jqsrt.2024.108906, 2024.

Diringer, S. E., Berky, A. J., Marani, M., Ortiz, E. J., Karatum, O., Plata, D. L., Pan, W. K., and Hsu-Kim, H.: Deforestation Due to Artisanal and Small-Scale Gold Mining Exacerbates Soil and Mercury Mobilization in Madre de Dios, Peru, Environ. Sci. Technol., 54, 286–296, https://doi.org/10.1021/acs.est.9b06620, 2020.

Dolce, C. H. H. and Miller, P. W.: Systematic Identification of Saharan Air Layer Events over the Tropical North Atlantic Ocean, J. Appl. Meteorol. Climatol., 64, 1343–1356, https://doi.org/10.1175/JAMC-D-24-0232.1, 2025.

Donarummo, J., Ram, M., and Stoermer, E. F.: Possible deposit of soil dust from the 1930's U.S. dust bowl identified in Greenland ice, Geophys. Res. Lett., 30, https://doi.org/10.1029/2002GL016641, 2003.

Doughty, P. L.: Plan and Pattern in Reaction to Earthquake: Peru, 1970-1998, in: The Angry Earth, Routledge, 248--270, 1999.

Emmer, A., Wood, J. L., Cook, S. J., Harrison, S., Wilson, R., Diaz-Moreno, A., Reynolds, J. M., Torres, J. C., Yarleque, C., Mergili, M., Jara, H. W., Bennett, G., Caballero, A., Glasser, N. F., Melgarejo, E., Riveros, C., Shannon, S., Turpo, E., Tinoco, T., Torres, L., Garay, D., Villafane, H., Garrido, H., Martinez, C., Apaza, N., Araujo, J., and Poma, C.: 160 glacial lake outburst floods (GLOFs) across the Tropical Andes since the Little Ice Age, Global Planet. Change, 208, 103722, https://doi.org/10.1016/j.gloplacha.2021.103722, 2022.

Engelbrecht, J. P. . and Derbyshire, E.: Airborne Mineral Dust, Elements, 6, 241–46, https://doi.org/10.2113/gselements.6.4.241, 2010.

Evan, A. and Mukhopadhyay, S.: African Dust over the Northern Tropical Atlantic: 1955–2008, J. Appl. Meteorol. Climatol., 49, 2213–2229, https://doi.org/10.1175/2010JAMC2485.1, 2010.

Fearnside, P. M.: Deforestation in Brazilian Amazonia: History, Rates, and Consequences, Conserv. Biol., 19, 680–688, https://doi.org/10.1111/j.1523-1739.2005.00697.x, 2005.

Flanner, M. G., Arnheim, J. B., Cook, J. M., Dang, C., He, C., Huang, X., Singh, D., Skiles, S. M., Whicker, C. A., and Zender, C. S.: SNICAR-ADv3: A community tool for modeling spectral snow albedo, Geosci. Model Dev., 14, 7673–7704, https://doi.org/10.5194/gmd-14-7673-2021, 2021.

Fortner, S. K., Mark, B. G., McKenzie, J. M., Bury, J., Trierweiler, A., Baraer, M., Burns, P. J., and Munk, L.: Elevated stream trace and minor element concentrations in the foreland of receding tropical glaciers, Appl. Geochem., 26, 1792–1801, https://doi.org/10.1016/j.apgeochem.2011.06.003, 2011.

Gaiero, D. m., Simonella, L., Gassó, S., Gili, S., Stein, A. f., Sosa, P., Becchio, R., Arce, J., and Marelli, H.: Ground/satellite observations and atmospheric modeling of dust storms originating in the high Puna-Altiplano deserts (South America): Implications for the interpretation of paleo-climatic archives, J. Geophys. Res.: Atmos., 118, 3817–3831, https://doi.org/10.1002/jgrd.50036, 2013.

Ganor, E.: The composition of clay minerals transported to Israel as indicators of Saharan dust emission, Atmos. Environ. Part A, 25, 2657–2664, https://doi.org/10.1016/0960-1686(91)90195-D, 1991.

https://doi.org/10.5194/egusphere-2026-3846
Preprint. Discussion started: 8 July 2026

Gassó, S., Grassian, V. H., and Miller, R. L.: Interactions between Mineral Dust, Climate, and Ocean Ecosystems, Elements, 6, 247–52, https://doi.org/10.2113/gselements.6.4.247, 2010.

Georges, C.: 20th-Century Glacier Fluctuations in the Tropical Cordillera Blanca, Perú, Arct. Antarct. Alp. Res., 36, 100–107, https://www.jstor.org/stable/1552433, 2004.

Gieré, R. and Querol, X.: Solid Particulate Matter in the Atmosphere, Elements, 6, 215–22, https://doi.org/10.2113/gselements.6.4.215, 2010.

Gilardoni, S., Di Mauro, B., and Bonasoni, P.: Black carbon, organic carbon, and mineral dust in South American tropical glaciers: A review, Global Planet. Change, 213, 103837, https://doi.org/10.1016/j.gloplacha.2022.103837, 2022.

Ginoux, P., Prospero, J. M., Gill, T. E., Hsu, N. C., and Zhao, M.: Global-scale attribution of anthropogenic and natural dust sources and their emission rates based on MODIS Deep Blue aerosol products, Rev. Geophys., 50, https://doi.org/10.1029/2012RG000388, 2012.

Giovanni, M. K., Horton, B. K., Garzione, C. N., McNulty, B., and Grove, M.: Extensional basin evolution in the Cordillera Blanca, Peru: Stratigraphic and isotopic records of detachment faulting and orogenic collapse in the Andean hinterland, Tectonics, 29, https://doi.org/10.1029/2010TC002666, 2010.

Glas, R., Lautz, L., McKenzie, J., Mark, B., Baraer, M., Chavez, D., and Maharaj, L.: A review of the current state of knowledge of proglacial hydrogeology in the Cordillera Blanca, Peru, WIREs Water, 5, e1299, https://doi.org/10.1002/wat2.1299, 2018.

Goldstein, J. I., Newbury, D. E., Echlin, P., Joy, D. C., Lyman, C. E., Lifshin, E., Sawyer, L., and Michael, J. R.: Scanning Electron Microscopy and X-ray Microanalysis, Springer US, Boston, MA, https://doi.org/10.1007/978-1-4615-0215-9, 2003.

Gonçalves Ageitos, M., Obiso, V., Miller, R. L., Jorba, O., Klose, M., Dawson, M., Balkanski, Y., Perlwitz, J., Basart, S., Di Tomaso, E., Escribano, J., Macchia, F., Montané, G., Mahowald, N. M., Green, R. O., Thompson, D. R., and Pérez García-Pando, C.: Modeling dust mineralogical composition: sensitivity to soil mineralogy atlases and their expected climate impacts, Atmos. Chem. Phys., 23, 8623–8657, https://doi.org/10.5194/acp-23-8623-2023, 2023.

Gorin, A. L., Shakun, J. D., Jones, A. G., Kennedy, T. M., Marcott, S. A., Goehring, B. M., Zoet, L. K., Jomelli, V., Bromley, G. R. M., Mateo, E. I., Mark, B. G., Rodbell, D. T., Gilbert, A., and Caffee, M. W.: Recent tropical Andean glacier retreat is unprecedented in the Holocene, Science, 385, 517–521, https://doi.org/10.1126/science.adg7546, 2024.

Groundwater, H., Twardowski, M. S., Dierssen, H. M., Sciandra, A., and Freeman, S. A.: Determining Size Distributions and Composition of Particles Suspended in Water: A New SEM–EDS Protocol with Validation and Comparison to Other Methods, J. Atmos. Oceanic Technol., 29, 433--449, https://doi.org/10.1175/JTECH-D-11-00026.1, 2012.

Guyot, J. L., Jouanneau, J. M., Soares, L., Boaventura, G. R., Maillet, N., and Lagane, C.: Clay mineral composition of river sediments in the Amazon Basin, CATENA, 71, 340–356, https://doi.org/10.1016/j.catena.2007.02.002, 2007.

Harvey, C.: One Third of the Amazon Has Been Degraded by Human Activities, Sci. Am., 2023.

Henderson, K. A., Thompson, L. G., and Lin, P.-N.: Recording of El Niño in ice core $\delta^{18}O$ records from Nevado Huascarán, Peru, J. Geophys. Res.: Atmos., 104, 31053–31065, https://doi.org/10.1029/1999JD900966, 1999.

https://doi.org/10.5194/egusphere-2026-3846
Preprint. Discussion started: 8 July 2026

Highwood, E. J. and Ryder, C. L.: Radiative Effects of Dust, in: Mineral Dust: A Key Player in the Earth System, edited by: Knippertz, P. and Stuut, J.-B. W., Springer Netherlands, Dordrecht, 267–286, https://doi.org/10.1007/978-94-017-8978-3_11, 2014.

Irion, G.: Clay minerals of Amazonian soils, in: The Amazon: Limnology and landscape ecology of a mighty tropical river and its basin, edited by: Sioli, H., Springer Netherlands, Dordrecht, 537–579, https://doi.org/10.1007/978-94-009-6542-3_21, 1984.

Kalamandeen, M., Gloor, E., Mitchard, E., Quincey, D., Ziv, G., Spracklen, D., Spracklen, B., Adami, M., Aragão, L. E. O. C., and Galbraith, D.: Pervasive Rise of Small-scale Deforestation in Amazonia, Sci. Rep., 8, 1600, https://doi.org/10.1038/s41598-018-19358-2, 2018.

Kalnay, E., Kanamitsu, M., Kistler, R., Collins, W., Deaven, D., Gandin, L., Iredell, M., Saha, S., White, G., Woollen, J., Zhu, Y., Chelliah, M., Ebisuzaki, W., Higgins, W., Janowiak, J., Mo, K. C., Ropelewski, C., Wang, J., Leetmaa, A., Reynolds, R., Jenne, R., and Joseph, D.: The NCEP/NCAR 40-Year Reanalysis Project, Bull. Am. Meteorol. Soc., 77, 437--472, https://doi.org/10.1175/1520-0477(1996)077<0437:TNYRP>2.0.CO;2, 1996.

Kandler, K., Lieke, K., Benker, N., Emmel, C., Küpper, M., Müller-Ebert, D., Ebert, M., Scheuvens, D., Schladitz, A., Schütz, L., and Weinbruch, S.: Electron microscopy of particles collected at Praia, Cape Verde, during the Saharan Mineral Dust Experiment: particle chemistry, shape, mixing state and complex refractive index, Tellus B, 63, 475–496, https://doi.org/10.1111/j.1600-0889.2011.00550.x, 2011.

Kaser, G., Juen, I., Georges, C., Gómez, J., and Tamayo, W.: The impact of glaciers on the runoff and the reconstruction of mass balance history from hydrological data in the tropical Cordillera Blanca, Perú, J. Hydrol., 282, 130–144, https://doi.org/10.1016/S0022-1694(03)00259-2, 2003.

Kok, J., Storelvmo, T., Karydis, V., Adebiyi, A., Mahowald, N., Evan, A., He, C., and Leung, D.: Mineral dust aerosol impacts on global climate and climate change, Nat. Rev. Earth Environ., 4, https://doi.org/10.1038/s43017-022-00379-5, 2023.

Koren, I., Kaufman, Y. J., Washington, R., Todd, M. C., Rudich, Y., Vanderlei Martins, J., and Rosenfeld, D.: The Bodélé depression: a single spot in the Sahara that provides most of the mineral dust to the Amazon forest, Environ. Res. Lett., 1, 014005, https://doi.org/10.1088/1748-9326/1/1/014005, 2006.

Kutuzov, S., Thompson, L. G., Bolzan, J. F., Lavrentiev, I., Chernyakov, G., and Schoessow, F.: A Geophysical and Glaciological Survey of the Highest Tropical Mountain glaciers (Mt. Huascarán, Andes), J. Glaciol., 71, 1–14, https://doi.org/10.1017/jog.2025.20, 2025.

Lapola, D. M., Pinho, P., Barlow, J., Aragão, L. E. O. C., Berenguer, E., Carmenta, R., Liddy, H. M., Seixas, H., Silva, C. V. J., Silva-Junior, C. H. L., Alencar, A. A. C., Anderson, L. O., Armenteras, D., Brovkin, V., Calders, K., Chambers, J., Chini, L., Costa, M. H., Faria, B. L., Fearnside, P. M., Ferreira, J., Gatti, L., Gutierrez-Velez, V. H., Han, Z., Hibbard, K., Koven, C., Lawrence, P., Pongratz, J., Portela, B. T. T., Rounsevell, M., Ruane, A. C., Schaldach, R., da Silva, S. S., von Randow, C., and Walker, W. S.: The drivers and impacts of Amazon forest degradation, Science, 379, eabp8622, https://doi.org/10.1126/science.abp8622, 2023.

Lavrent'ev, Y. G., Karmanov, N. S., and Usova, L. V.: Electron probe microanalysis of minerals: Microanalyzer or scanning electron microscope?, Russ. Geol. Geophys., 56, 1154--1161, https://doi.org/10.1016/j.rgg.2015.07.006, 2015.

Leite-Filho, A. T., Soares-Filho, B. S., Davis, J. L., Abrahão, G. M., and Börner, J.: Deforestation reduces rainfall and agricultural revenues in the Brazilian Amazon, Nat. Commun., 12, 2591, https://doi.org/10.1038/s41467-021-22840-7, 2021.

https://doi.org/10.5194/egusphere-2026-3846
Preprint. Discussion started: 8 July 2026

Li, J. and Osada, K.: Preferential settling of elongated mineral dust particles in the atmosphere, Geophys. Res. Lett., 34, https://doi.org/10.1029/2007GL030262, 2007.

Lindau, F. G. L., Simões, J. C., Delmonte, B., Ginot, P., Baccolo, G., Paleari, C. I., Di Stefano, E., Korotkikh, E., Introne, D. S., Maggi, V., Garzanti, E., and Andò, S.: Giant dust particles at Nevado Illimani: a proxy of summertime deep convection over the Bolivian Altiplano, The Cryosphere, 15, 1383–1397, https://doi.org/10.5194/tc-15-1383-2021, 2021.

Lovejoy, T. E. and Nobre, C.: Amazon Tipping Point, Sci. Adv., 4, https://doi.org/10.1126/sciadv.aat2340, 2018.

Maggi, V.: Mineralogy of atmospheric microparticles deposited along the Greenland Ice Core Project ice core, J. Geophys. Res.: Oceans, 102, 26725–26734, https://doi.org/10.1029/97JC00613, 1997.

Magnússon, R., Cammeraat, E., Lücke, A., Jansen, B., Zimmer, A., and Recharte, J.: Influence of glacial sediments on the chemical quality of surface water in the Ulta valley, Cordillera Blanca, Peru, J. Hydrol., 587, 125027, https://doi.org/10.1016/j.jhydrol.2020.125027, 2020.

Malhi, Y., Roberts, J. T., Betts, R. A., Killeen, T. J., Li, W., and Nobre, C. A.: Climate Change, Deforestation, and the Fate of the Amazon, Science, 319, 169–172, https://doi.org/10.3832/efor0516-005, 2008.

Mark, B. G., Stansell, N. D., Shutkin, T., and Schoessow, F.: Glaciation and the Environments of the Cordillera Blanca, in: Geoenvironmental Changes in the Cordillera Blanca, Peru, edited by: Vilímek, V., Mark, B., and Emmer, A., Springer International Publishing, Cham, 95–115, https://doi.org/10.1007/978-3-031-58245-5_6, 2024.

McGregor, S., Stuecker, M. F., Kajtar, J. B., England, M. H., and Collins, M.: Model tropical Atlantic biases underpin diminished Pacific decadal variability, Nature Clim. Change, 8, 493–498, https://doi.org/10.1038/s41558-018-0163-4, 2018.

Meinander, O., Dagsson-Waldhauserova, P., Amosov, P., Aseyeva, E., Atkins, C., Baklanov, A., Baldo, C., Barr, S. L., Barzycka, B., Benning, L. G., Cvetkovic, B., Enchilik, P., Frolov, D., Gassó, S., Kandler, K., Kasimov, N., Kavan, J., King, J., Koroleva, T., Krupskaya, V., Kulmala, M., Kusiak, M., Lappalainen, H. K., Laska, M., Lasne, J., Lewandowski, M., Luks, B., McQuaid, J. B., Moroni, B., Murray, B., Möhler, O., Nawrot, A., Nickovic, S., O'Neill, N. T., Pejanovic, G., Popovicheva, O., Ranjbar, K., Romanias, M., Samonova, O., Sanchez-Marroquin, A., Schepanski, K., Semenkov, I., Sharapova, A., Shevnina, E., Shi, Z., Sofiev, M., Thevenet, F., Thorsteinsson, T., Timofeev, M., Umo, N. S., Uppstu, A., Urupina, D., Varga, G., Werner, T., Arnalds, O., and Vukovic Vimic, A.: Newly identified climatically and environmentally significant high-latitude dust sources, Atmos. Chem. Phys., 22, 11889–11930, https://doi.org/10.5194/acp-22-11889-2022, 2022.

Menéndez, I., Díaz-Hernández, J. L., Mangas, J., Alonso, I., and Sánchez-Soto, P. J.: Airborne dust accumulation and soil development in the North-East sector of Gran Canaria (Canary Islands, Spain), J. Arid. Environ., 71, 57–81, https://doi.org/10.1016/j.jaridenv.2007.03.011, 2007.

Menéndez, I., Pérez-Chacón, E., Mangas, J., Tauler, E., Engelbrecht, J. P., Derbyshire, E., Cana, L., and Alonso, I.: Dust deposits on La Graciosa Island (Canary Islands, Spain): Texture, mineralogy and a case study of recent dust plume transport, CATENA, 117, 133–144, https://doi.org/10.1016/j.catena.2013.05.007, 2014.

Michaud, A. B., Dore, J. E., Leslie, D., Lyons, W. B., Sands, D. C., and Priscu, J. C.: Biological ice nucleation initiates hailstone formation, J. Geophys. Res.: Atmos., 119, 12,186-12,197, https://doi.org/10.1002/2014JD022004, 2014.

Montini, T. L., Jones, C., and Carvalho, L. M. V.: The South American Low-Level Jet: A New Climatology, Variability, and Changes, J. Geophys. Res.: Atmos., 124, 1200–1218, https://doi.org/10.1029/2018JD029634, 2019.

https://doi.org/10.5194/egusphere-2026-3846
Preprint. Discussion started: 8 July 2026

Moreno, T., Querol, X., Castillo, S., Alastuey, A., Cuevas, E., Herrmann, L., Mounkaila, M., Elvira, J., and Gibbons, W.: Geochemical variations in aeolian mineral particles from the Sahara–Sahel Dust Corridor, Chemosphere, 65, 261–270, https://doi.org/10.1016/j.chemosphere.2006.02.052, 2006.

Motschmann, A., Huggel, C., Carey, M., Moulton, H., Walker-Crawford, N., and Muñoz, R.: Losses and damages connected to glacier retreat in the Cordillera Blanca, Peru, Clim. Change, 162, 837–858, https://doi.org/10.1007/s10584-020-02770-x, 2020.

Mounkaila, M.: Spectral and mineralogical properties of potential dust sources on a transect from the Bodélé Depression (Central Sahara) to the Lake Chad in the Sahel, Ph.D. thesis, Universität Hohenheim, Germany, 2006.

Mu, Y. and Jones, C.: An observational analysis of precipitation and deforestation age in the Brazilian Legal Amazon, Atmos. Res., 271, 106122, https://doi.org/10.1016/j.atmosres.2022.106122, 2022.

Muhs, D. R., Prospero, J. M., Baddock, M. C., and Gill, T. E.: Identifying Sources of Aeolian Mineral Dust: Present and Past, in: Mineral Dust: A Key Player in the Earth System, edited by: Knippertz, P. and Stuut, J.-B. W., Springer Netherlands, Dordrecht, 51–74, https://doi.org/10.1007/978-94-017-8978-3_3, 2014.

Nagatsuka, N., Goto-Azuma, K., Tsushima, A., Fujita, K., Matoba, S., Onuma, Y., Dallmayr, R., Kadota, M., Hirabayashi, M., Ogata, J., Ogawa-Tsukagawa, Y., Kitamura, K., Minowa, M., Komuro, Y., Motoyama, H., and Aoki, T.: Variations in mineralogy of dust in an ice core obtained from northwestern Greenland over the past 100 years, Clim. Past, 17, 1341–1362, https://doi.org/10.5194/cp-17-1341-2021, 2021.

NGDC: ETOPO2, Global 2 Arc-minute Ocean Depth and Land Elevation from the US National Geophysical Data Center (NGDC), GDEX.UCAR.edu [data set], https://doi.org/10.5065/D6668B75, 2001.

Nobre, C. A., Sellers, P. J., and Shukla, J.: Amazonian Deforestation and Regional Climate Change, J. Clim., 4, 957–988, https://doi.org/10.1175/1520-0442(1991)004%3C0957:ADARCC%3E2.0.CO;2, 1991.

Nowak, S., Lafon, S., Caquineau, S., Journet, E., and Laurent, B.: Quantitative study of the mineralogical composition of mineral dust aerosols by X-ray diffraction, Talanta, 186, 133–139, https://doi.org/10.1016/j.talanta.2018.03.059, 2018.

Okada, K., Heintzenberg, J., Kai, K., and Qin, Y.: Shape of atmospheric mineral particles collected in three Chinese arid-regions, Geophys. Res. Lett., 28, 3123–3126, https://doi.org/10.1029/2000GL012798, 2001.

Olmo, M. E., Espinoza, J.-C., Bettolli, M. L., Sierra, J. P., Junquas, C., Arias, P. A., Moron, V., and Balmaceda-Huarte, R.: Circulation Patterns and Associated Rainfall Over South Tropical South America: GCMs Evaluation During the Dry-To-Wet Transition Season, J. Geophys. Res.: Atmos., 127, e2022JD036468, https://doi.org/10.1029/2022JD036468, 2022.

Osterberg, E. C., Handley, M. J., Sneed, S. B., Mayewski, P. A., and Kreutz, K. J.: Continuous Ice Core Melter System with Discrete Sampling for Major Ion, Trace Element, and Stable Isotope Analyses, Environ. Sci. Technol., 40, 3355–3361, https://doi.org/10.1021/es052536w, 2006.

Painter, T. H., Barrett, A. P., Landry, C. C., Neff, J. C., Cassidy, M. P., Lawrence, C. R., McBride, K. E., and Farmer, G. L.: Impact of disturbed desert soils on duration of mountain snow cover, Geophys. Res. Lett., 34, https://doi.org/10.1029/2007GL030284, 2007.

Panta, A., Kandler, K., Alastuey, A., González-Flórez, C., González-Romero, A., Klose, M., Querol, X., Reche, C., Yus-Díez, J., and Pérez García-Pando, C.: Insights into the single-particle composition, size, mixing state, and aspect ratio of

https://doi.org/10.5194/egusphere-2026-3846
Preprint. Discussion started: 8 July 2026

freshly emitted mineral dust from field measurements in the Moroccan Sahara using electron microscopy, Atmos. Chem. Phys., 23, 3861–3885, https://doi.org/10.5194/acp-23-3861-2023, 2023.

Pawlowicz, R.: M_Map: A mapping package for MATLAB, www.eoas.ubc.ca/~rich/map.html, 2020.

Permana, D. S., Thompson, L. G., Mosley-Thompson, E., Davis, M. E., Lin, P.-N., Nicolas, J. P., Bolzan, J. F., Bird, B. W., Mikhalenko, V. N., Gabrielli, P., Zagorodnov, V., Mountain, K. R., Schotterer, U., Hanggoro, W., Habibie, M. N., Kaize, Y., Gunawan, D., Setyadi, G., Susanto, R. D., Fernández, A., and Mark, B. G.: Disappearance of the last tropical glaciers in the Western Pacific Warm Pool (Papua, Indonesia) appears imminent, Proc. Natl. Acad. Sci. U.S.A., 116, 26382–26388, https://doi.org/10.1073/pnas.1822037116, 2019.

Petford, N. and Atherton, M.: Na-rich Partial Melts from Newly Underplated Basaltic Crust: the Cordillera Blanca Batholith, Peru, J. Petrol., 37, 1491–1521, https://doi.org/10.1093/petrology/37.6.1491, 1996.

Petit, R. H., Legrand, M., Jankowiak, I., Molinié, J., Asselin de Beauville, C., Marion, G., and Mansot, J. L.: Transport of Saharan dust over the Caribbean Islands: Study of an event, J. Geophys. Res.: Atmos., 110, https://doi.org/10.1029/2004JD004748, 2005.

Plafker, G. and Ericksen, G. E.: Nevados Huascarán Avalanches, Peru, in: Developments in Geotechnical Engineering, vol. 14A, Elsevier, 277–314, https://doi.org/10.1016/B978-0-444-41507-3.50016-7, 1978.

Plafker, G., Ericksen, G. E., and Fernández Concha, J.: Geological aspects of the May 31, 1970, Perú earthquake, Bull. Seismol. Soc. Am., 61, 543--578, https://doi.org/10.1785/bssa0610030543, 1971.

Poveda, G.: Critical Slowing Down Reveals Hydrologic Resilience Loss Across Amazon Sub-Basins, Water Resour. Res., 62, e2025WR040039, https://doi.org/10.1029/2025WR040039, 2026.

PRODES: Monitoring deforestation of the Brazilian Amazon rainforest by satellite [data set], http://www.obt.inpe.br/OBT/assuntos/programas/amazonia/prodes, last access: 3 April 2021, 2020.

Prospero, J. M., Glaccum, R. A., and Nees, R. T.: Atmospheric transport of soil dust from Africa to South America, Nature, 289, 570–572, https://doi.org/10.1038/289570a0, 1981.

Prospero, J. M., Barkley, A. E., Gaston, C. J., Gatineau, A., Sansano, A. C. y, and Panechou, K.: Characterizing and Quantifying African Dust Transport and Deposition to South America: Implications for the Phosphorus Budget in the Amazon Basin, Global Biogeochem. Cycles, 34, e2020GB006536, https://doi.org/10.1029/2020GB006536, 2020.

Prospero, J. M., Delany, A. C., Delany, A. C., and Carlson, T. N.: The Discovery of African Dust Transport to the Western Hemisphere and the Saharan Air Layer: A History, Bull. Am. Meteorol. Soc., 102, E1239–E1260, https://doi.org/10.1175/BAMS-D-19-0309.1, 2021.

Pye, K.: Shape Sorting During Wind Transport of Quartz Silt Grains: Discussion, J. Sediment. Res., A64, 704--705, 1994.

Ramirez, E., Hoffmann, G., Taupin, J. D., Francou, B., Ribstein, P., Caillon, N., Ferron, F. A., Landais, A., Petit, J. R., Pouyaud, B., Schotterer, U., Simoes, J. C., and Stievenard, M.: A new Andean deep ice core from Nevado Illimani (6350 m), Bolivia, Earth Planet. Sci. Lett., 212, 337–350, https://doi.org/10.1016/S0012-821X(03)00240-1, 2003.

Reid, J. S., Jonsson, H. H., Maring, H. B., Smirnov, A., Savoie, D. L., Cliff, S. S., Reid, E. A., Livingston, J. M., Meier, M. M., Dubovik, O., and Tsay, S.-C.: Comparison of size and morphological measurements of coarse mode dust particles from Africa, J. Geophys. Res.: Atmos., 108, https://doi.org/10.1029/2002JD002485, 2003.

https://doi.org/10.5194/egusphere-2026-3846
Preprint. Discussion started: 8 July 2026

Restrepo-Coupe, N., O'Donnell Christoffersen, B., Longo, M., Alves, L. F., Campos, K. S., da Araujo, A. C., de Oliveira Jr, R. C., Prohaska, N., da Silva, R., Tapajos, R., Wiedemann, K. T., Wofsy, S. C., and Saleska, S. R.: Asymmetric response of Amazon forest water and energy fluxes to wet and dry hydrological extremes reveals onset of a local drought-induced tipping point, Global Change Biol., 29, 6077–6092, https://doi.org/10.1111/gcb.16933, 2023.

RGI Consortium: Randolph Glacier Inventory - A Dataset of Global Glacier Outlines. (NSIDC-0770, Version 7) [data set], https://doi.org/10.5067/F6JMOVY5NAVZ, 2023.

Ro, S., Park, J., Yoo, H., Han, C., Lee, A., Lee, Y., Kim, M., Han, Y., Svensson, A., Shin, J., Ro, C.-U., and Hong, S.: Millennial-scale variability of Greenland dust provenance during the last glacial maximum as determined by single particle analysis, Sci. Rep., 14, 2040, https://doi.org/10.1038/s41598-024-52546-x, 2024.

Rodriguez-Navarro, C., di Lorenzo, F., and Elert, K.: Mineralogy and physicochemical features of Saharan dust wet deposited in the Iberian Peninsula during an extreme red rain event, Atmos. Chem. Phys., 18, 10089–10122, https://doi.org/10.5194/acp-18-10089-2018, 2018.

Rojas Briceño, N. B., Castillo, E. B., Maicelo Quintana, J. L., Oliva Cruz, S. M., and Salas Lopez, R.: Deforestation in the Peruvian Amazon: indices of land cover and land use changes based on GIS, BAGE, 81, https://doi.org/10.21138/bage.2538a, 2019.

Rosales, A. G., Junquas, C., da Rocha, R. P., Condom, T., and Espinoza, J.-C.: Valley–Mountain Circulation Associated with the Diurnal Cycle of Precipitation in the Tropical Andes (Santa River Basin, Peru), Atmosphere, 13, 344, https://doi.org/10.3390/atmos13020344, 2022.

Rostási, Á., Topa, B. A., Gresina, F., Weiszburg, T. G., Gelencsér, A., and Varga, G.: Saharan Dust Deposition in Central Europe in 2016—A Representative Year of the Increased North African Dust Removal Over the Last Decade, Front. Earth Sci., 10, https://doi.org/10.3389/feart.2022.869902, 2022.

Royer, A., De Angelis, M., and Petit, J. R.: A 30000 year record of physical and optical properties of microparticles from an East Antarctic ice core and implications for paleoclimate reconstruction models, Clim. Change, 5, 381–412, https://doi.org/10.1007/BF00140802, 1983.

Sánchez Rodríguez, W. and Schmitt, C.: Partículas Absorbentes de Luz durante El Niño y El Niño Costero en los Glaciares de la Cordillera Blanca, Perú [Light-absorbing Particles during El Niño and El Niño Costero in the Glaciers of the Cordillera Blanca, Peru], REVISTA, 4, 9–22, https://doi.org/10.36580/rgem.i4.9-22, 2018.

Sardans, J., Miralles, A., Tariq, A., Zeng, F., Wang, R., and Peñuelas, J.: Growing aridity poses threats to global land surface, Commun. Earth Environ., 5, 776, https://doi.org/10.1038/s43247-024-01935-1, 2024.

Scheuvens, D., Schütz, L., Kandler, K., Ebert, M., and Weinbruch, S.: Bulk composition of northern African dust and its source sediments — A compilation, Earth Sci. Rev., 116, 170–194, https://doi.org/10.1016/j.earscirev.2012.08.005, 2013.

Schimmenti, D. E., Marcantonio, F., Roxana Sierra-Hernández, M., and Schmidt, M. W.: Millennial pulses of African dust and ITCZ shifts in the Eastern Equatorial Pacific, Nat. Commun., 16, 5567, https://doi.org/10.1038/s41467-025-60773-7, 2025.

Schindelin, J., Arganda-Carreras, I., Frise, E., Kaynig, V., Longair, M., Pietzsch, T., Preibisch, S., Rueden, C., Saalfeld, S., Schmid, B., Tinevez, J.-Y., White, D. J., Hartenstein, V., Eliceiri, K., Tomancak, P., and Cardona, A.: Fiji: an open-source platform for biological-image analysis, Nat. Methods, 9, 676–682, https://doi.org/10.1038/nmeth.2019, 2012.

https://doi.org/10.5194/egusphere-2026-3846
Preprint. Discussion started: 8 July 2026

Schmitt, C. G., All, J. D., Schwarz, J. P., Arnott, W. P., Cole, R. J., Lapham, E., and Celestian, A.: Measurements of light-absorbing particles on the glaciers in the Cordillera Blanca, Peru, The Cryosphere, 9, 331–340, https://doi.org/10.5194/tc-9-331-2015, 2015.

Schoessow, F. S.: Dynamics of Modern Deglaciation Across Earth's Highest Tropical Mountains, Ph.D. thesis, The Ohio State University, USA, http://rave.ohiolink.edu/etdc/view?acc_num=osu1746465938897616, 2025.

Schroeder, P. A. and Erickson, G.: Kaolin: From Ancient Porcelains to Nanocomposites, Elements, 10, 177–182, https://doi.org/10.2113/gselements.10.3.177, 2014.

Severin, K. P.: Energy Dispersive Spectrometry of Common Rock Forming Minerals, Kluwer Academic Publishers, Dordrecht, the Netherlands, https://doi.org/10.1007/978-1-4020-2841-0, 2004.

Shi, T., Cui, J., Chen, Y., Zhou, Y., Pu, W., Xu, X., Chen, Q., Zhang, X., and Wang, X.: Enhanced light absorption and reduced snow albedo due to internally mixed mineral dust in grains of snow, Atmos. Chem. Phys., 21, 6035–6051, https://doi.org/10.5194/acp-21-6035-2021, 2021.

Shugar, D. H., Clague, J. J., Best, J. L., Schoof, C., Willis, M. J., Copland, L., and Roe, G. H.: River piracy and drainage basin reorganization led by climate-driven glacier retreat, Nature Geosci., 10, 370–375, https://doi.org/10.1038/ngeo2932, 2017.

Sierra-Hernández, M. R., Marcantonio, F., Griffith, E. M., and Thompson, L. G.: Sources of lead in a Tibetan glacier since the Stone Age, Commun. Earth Environ., 5, 1–12, https://doi.org/10.1038/s43247-024-01724-w, 2024.

Silva Junior, C. H. L., Pessôa, A. C. M., Carvalho, N. S., Reis, J. B. C., Anderson, L. O., and Aragão, L. E. O. C.: The Brazilian Amazon deforestation rate in 2020 is the greatest of the decade, Nat. Ecol. Evol., 5, 144–145, https://doi.org/10.1038/s41559-020-01368-x, 2021.

Staal, A., Flores, B. M., Aguiar, A. P. D., Bosmans, J. H. C., Fetzer, I., and Tuinenburg, O. A.: Feedback between drought and deforestation in the Amazon, Environ. Res. Lett., 15, 044024, https://doi.org/10.1088/1748-9326/ab738e, 2020.

Stanelle, T., Bey, I., Raddatz, T., Reick, C., and Tegen, I.: Anthropogenically induced changes in twentieth century mineral dust burden and the associated impact on radiative forcing, J. Geophys. Res.: Atmos., 119, 13,526-13,546, https://doi.org/10.1002/2014JD022062, 2014.

Stein, A. F., Draxler, R. R., Rolph, G. D., Stunder, B. J. B., Cohen, M. D., and Ngan, F.: NOAA's HYSPLIT Atmospheric Transport and Dispersion Modeling System, Bull. Am. Meteorol. Soc., 96, 2059–2077, https://doi.org/10.1175/BAMS-D-14-00110.1, 2015.

Stuart-Smith, R. F., Roe, G. H., Li, S., and Allen, M. R.: Increased outburst flood hazard from Lake Palcacocha due to human-induced glacier retreat, Nat. Geosci., 14, 85–90, https://doi.org/10.1038/s41561-021-00686-4, 2021.

Svensson, A., Biscaye, P. E., and Grousset, F. E.: Characterization of late glacial continental dust in the Greenland Ice Core Project ice core, J. Geophys. Res., 105, https://doi.org/http://rave.ohiolink.edu/ejournals/article/360412876, 2000.

Taylor, C., Robinson, T. R., Dunning, S., Rachel Carr, J., and Westoby, M.: Glacial lake outburst floods threaten millions globally, Nat. Commun., 14, 487, https://doi.org/10.1038/s41467-023-36033-x, 2023.

Tegen, I. and Fung, I.: Contribution to the atmospheric mineral aerosol load from land surface modification, J. Geophys. Res.: Atmos., 100, 18707–18726, https://doi.org/10.1029/95JD02051, 1995.

https://doi.org/10.5194/egusphere-2026-3846
Preprint. Discussion started: 8 July 2026

Tegen, I. and Schulz, M.: Numerical Dust Models, in: Mineral Dust: A Key Player in the Earth System, edited by: Knippertz, P. and Stuut, J.-B. W., Springer Netherlands, Dordrecht, 201–222, https://doi.org/10.1007/978-94-017-8978-3_9, 2014.

Tegen, I., Lacis, A. A., and Fung, I.: The influence on climate forcing of mineral aerosols from disturbed soils, Nature, 380, 419–422, https://doi.org/10.1038/380419a0, 1996.

Thompson, L. G., Mosley-Thompson, E., Davis, M. E., Lin, P.-N., Henderson, K. A., Cole-Dai, J., Bolzan, J. F., and Liu, K. -b.: Late Glacial Stage and Holocene tropical ice core records from Huascarán, Peru, Science, 269, 46--50, https://doi.org/10.1126/science.269.5220.46, 1995.

Thompson, L. G., Davis, M. E., Mosley-Thompson, E., Sowers, T. A., Henderson, K. A., Zagorodnov, V. S., Lin, P.-N., Mikhalenko, R. K., Campen, R. K., Bolzan, J. F., Cole-Dai, J., and Francou, B.: A 25,000-Year Tropical Climate History from Bolivian Ice Cores, Science, 282, 1858–1864, https://doi.org/10.1126/science.282.5395.1858, 1998.

Thompson, L. G., Mosley-Thompson, E., Davis, M. E., Henderson, K. A., Brecher, H. H., Zagorodnov, V. S., Mashiotta, T. A., Lin, P.-N., Mikhalenko, V. N., Hardy, D. R., and Beer, J.: Kilimanjaro Ice Core Records: Evidence of Holocene Climate Change in Tropical Africa, Science, 298, 589–593, https://doi.org/10.1126/science.1073198, 2002.

Thompson, L. G., Mosley-Thompson, E., Davis, M. E., Zagorodnov, V. S., Howat, I. M., Mikhalenko, V. N., and Lin, P.-N.: Annually Resolved Ice Core Records of Tropical Climate Variability over the Past 1800 Years, Science, 340, 945–950, https://doi.org/10.1126/science.1234210, 2013.

Thompson, L. G., Davis, M. E., Mosley-Thompson, E., Porter, S. E., Corrales, G. V., Shuman, C. A., and Tucker, C. J.: The impacts of warming on rapidly retreating high-altitude, low-latitude glaciers and ice core-derived climate records, Global Planet. Change, 203, 103538, https://doi.org/10.1016/j.gloplacha.2021.103538, 2021.

Tomadin, L. and Lenaz, R.: Eolian Dust over the Mediterranean and Their Contribution to the Present Sedimentation, in: Paleoclimatology and Paleometeorology: Modern and Past Patterns of Global Atmospheric Transport, edited by: Leinen, M. and Sarnthein, M., Springer Netherlands, Dordrecht, 267–282, https://doi.org/10.1007/978-94-009-0995-3_11, 1989.

Van Der Does, M., Knippertz, P., Zschenderlein, P., Giles Harrison, R., and Stuut, J.-B. W.: The mysterious long-range transport of giant mineral dust particles, Sci. Adv., 4, eaau2768, https://doi.org/10.1126/sciadv.aau2768, 2018.

Vuille, M., Kaser, G., and Juen, I.: Glacier mass balance variability in the Cordillera Blanca, Peru and its relationship with climate and the large-scale circulation, Global Planet. Change, 62, 14–28, https://doi.org/10.1016/j.gloplacha.2007.11.003, 2008.

Warren, S. G.: Impurities in Snow: Effects on Albedo and Snowmelt (Review), Ann. Glaciol., 5, 177–179, https://doi.org/10.3189/1984AoG5-1-177-179, 1984.

Weber, A. M.: Algorithms for SEM-EDS Mineral Dust Classification, J. Open Source Software, 10, 7533, https://doi.org/10.21105/joss.07533, 2025.

Weber, A. M.: Code used for analysis and visualization in “Ice core insights into the morphology and composition of mineral dust deposited in the tropical Peruvian Andes”, Zenodo [code], https://doi.org/10.5281/zenodo.20817171, 2026

Weber, A. M., Thompson, L. G., Davis, M., Mosley-Thompson, E., Beaudon, E., Kenny, D., Lin, P.-N., and Sierra-Hernández, R.: Drivers of $\delta^{18}O$ Variability Preserved in Ice Cores From Earth’s Highest Tropical Mountain, J. Geophys. Res.: Atmos., 128, e2023JD039006, https://doi.org/10.1029/2023JD039006, 2023.

https://doi.org/10.5194/egusphere-2026-3846
Preprint. Discussion started: 8 July 2026

Weber, A. M., Beaudon, E., Sierra-Hernández, M. R., Davis, M., Kenny, D., Shutkin, T. Y., and Thompson, L. G.: On the Influence of Mineral Dust on Glacial Albedo at Nevado Huascarán (Cordillera Blanca, Peru), J. Geophys. Res.: Atmos., 131, e2025JD045574, https://doi.org/10.1029/2025JD045574, 2026a.

Weber, A. M., Kutuzov, S., Beaudon, E., Sierra-Hernández, M. R., Davis, M., Bayless, L. H., Kenny, D., and Thompson, L. G.: Nevado Huascarán Ice Core Dust Morphology and Mineralogy 1960-2018 CE [data set], https://doi.org/10.25921/1j1e-tf69, 2026b.

Wiese, J., Becker, M., Yorath, G., and O'Connor, C.: An investigation into the relationship between particle shape and entrainment, Miner. Eng., 83, 211–216, https://doi.org/10.1016/j.mineng.2015.09.012, 2015.

Wu, G., Zhang, X., Zhang, C., and Xu, T.: Mineralogical and morphological properties of individual dust particles in ice cores from the Tibetan Plateau, J. Glaciol., 62, 46–53, https://doi.org/10.1017/jog.2016.8, 2016.

Xi, Y., Xu, C., Downey, A., Stevens, R., Bachelder, J. O., King, J., Hayes, P. L., and Bertram, A. K.: Ice nucleating properties of airborne dust from an actively retreating glacier in Yukon, Canada, Environ. Sci.: Atmos., 2, 714–726, https://doi.org/10.1039/D1EA00101A, 2022.

Yarleque, C.: Climate of the Cordillera Blanca, in: Geoenvironmental Changes in the Cordillera Blanca, Peru, edited by: Vilímek, V., Mark, B., and Emmer, A., Springer International Publishing, Cham, 41–59, https://doi.org/10.1007/978-3-031-58245-5_3, 2024.

Yeo, K., Oluleye, A., Yoroba, F., Hamidi, M., and Shao, Y.: Trend of North African Dust Storms and Potential Link to Climate Change, J. Geophys. Res.: Atmos., 131, e2025JD043630, https://doi.org/10.1029/2025JD043630, 2026.

Yu, H., Chin, M., Yuan, T., Bian, H., Remer, L. A., Prospero, J. M., Omar, A., Winker, D., Yang, Y., Zhang, Y., Zhang, Z., and Zhao, C.: The fertilizing role of African dust in the Amazon rainforest: A first multiyear assessment based on data from Cloud-Aerosol Lidar and Infrared Pathfinder Satellite Observations, Geophys. Res. Lett., 42, 1984–1991, https://doi.org/https://doi.org/10.1002/2015GL063040, 2015.

Yu, Y., Kalashnikova, O. V., Garay, M. J., Lee, H., Notaro, M., Campbell, J. R., Marquis, J., Ginoux, P., and Okin, G. S.: Disproving the Bodélé Depression as the Primary Source of Dust Fertilizing the Amazon Rainforest, Geophys. Res. Lett., 47, e2020GL088020, https://doi.org/10.1029/2020GL088020, 2020.

Zemp, D. C., Schleussner, C.-F., Barbosa, H. M. J., van der Ent, R. J., Donges, J. F., Heinke, J., Sampaio, G., and Rammig, A.: On the importance of cascading moisture recycling in South America, Atmos. Chem. Phys., 14, 13337–13359, https://doi.org/10.5194/acp-14-13337-2014, 2014.